Investigation on formability behavior of Al-TiB_2 composite material

A thesis submitted by

Endalew Tigabie Lakew

(GSR/0083/09)

Advisor: Dr. Desalegn Wogaso (Assistant Professor)

For the Partial fulfillment of the

Requirement for the award of degree

Of

Master of Science

In Manufacturing Engineering

Mechanical Design & Manufacturing Engineering Program

School of Mechanical, Chemical and Materials Engineering

Adama Science and Technology University

March, 2019

ADAMA, ETHIOPIA

ADAMA SCIENCE AND TECHNOLOGY UNIVERSITY

School of Mechanical Chemical and Materials Engineering

Mechanical Design and Manufacturing Engineering Program

Adama, Ethiopia

Investigation on formability behavior of Al-TiB_2 composite material

By

Endalew Tigabie Lakew

Approved by board of examines

I. Chair, department graduate committee	Signature	Date
__________________________________	_________	_____________
II. Advisor	Signature	Date
__________________________________	__________	_____________
III. Internal examiner	Signature	Date
__________________________________	__________	_____________
IV. External examiner	Signature	Date
__________________________________	___________	_____________

DECLARATION

I hereby declare that the work which is being presented in this thesis entitled **"Investigation on formability behavior of Al-TiB_2 composite** submitted in partial fulfillment of the requirement for the award of the degree of Masters of Science in Manufacturing Engineering is my own work under the supervision of **Dr. Desalegn Wogaso**, program of Mechanical Design and Manufacturing Engineering, Adama Science and Technology University, Adama, Ethiopia.

The matter embodied in this thesis has not been submitted by me for the award of any other degree or diploma. All relevant resources of information used in this thesis have been duly acknowledged.

Endalew Tigabie Lakew   ID NO: GSR/0083/09   ______________   _____________

Candidate   Signature   Date

This is to certify that the above declaration made by the candidate is correct to the best of my knowledge and belief. This thesis has been submitted for examination with my approval.

Dr. Desalegn Wogaso   ______________   _______________

Advisor   Signature   Date

ACKNOWLEDGEMENT

First of all my deep gratitude goes to the almighty GOD for everything he did to me in all the way I path through, then after thanks for my adviser Dr. Desalegn W. including Mechanical design and Manufacturing engineering department staff members for their continues and progressive support, advice and guide me to do better work and give me a reference materials and initiate me for my work. In addition, I would like to thank also other local companies, which help in this work and their employees for their respect, familiarity, their advice and support. In addition, I would like to thank our classmates and friends for sharing their ideas and materials. Finally, I would like to thank our families for understanding and helping me with all my needs.

ABSTRACT

This study is focused on furthering our understanding of the different Titanium diboride percentage compositions that influence the formability of Aluminum- Titanium diboride (Al-TiB_2) composite materials. Formability is the ability of a given material to undergo plastic deformation without being damaged. The plastic deformation capacity of materials, however, is limited to a certain extent at which the material could experience fracture; thus, its investigation is critical for successful processing of materials during bulk deformation. The present investigation had been undertaken to evaluate the formability of Al-TiB_2 composites for pure Aluminum and various percentage TiB_2 powder compositions such as (0%, 4%, 8%, and 12%). In most production factories there is a great challenge or problem needs lightweight and high strength material, especially used in aerospace, automotive, and marine. Al with TiB_2 composite material is used to minimize this problem. This work mainly studies investigation of the formability behavior of Aluminum Titanium diboride composite material with various percentage compositions produced by using stir casting and using different mechanical tests specially compression test and micro structure and also numerical analysis by with DEFORM software. Mainly, this work studied and analyzed under formability experiment, must study compression test to generate the forming limit of the material and view stress-strain curve. It has been used as a reference to estimate how the material close to failure. The compression strength will estimate using a computerized universal testing machine. Basically Al –TiB_2 (8% TiB_2) is best from other composition i.e. 0% TiB_2, 4% TiB_2, 12% TiB_2. Since, if the ceramic powder or the reinforcement was more, the property of the material would change from ductile in to brittle. So, as we have seen the result Al –TiB_2 (8% TiB_2) composite material is best to forming process.

Key word: *Al-TiB_2 composite material, stir casting, formability, compression test*

TABLE OF CONTENT

Contents page

LIST OF FIGURES

LIST OF TABLES

ABBREVIATION AND NOMENCLATURE

Al	Aluminum
B_4C	Borne Carbide
FCC	Face Centered Cubic

FEM	Finite Element Method
Fe_3C	Iron Carbide
FLD	Forming Limit Diagram
FSP	Friction Stir Processing
MMCs	Metal Matrix Composites
Mo_2C	Molubdium Carbide
PM	Powder Metallurgy
SEM	Scanning Electron Microscope
TiB_2	Titanium diboride
TiC	Titanium Carbide
Vol	Volume
Wt	Weight
WC	Tungsten Carbide
Zn	Zinc
µm	micro meter

CHAPTER ONE

1. INTRODUCTION

1.1 Background and description

Aluminum has been known as the most common metal on earth. It is the third most abundant element. Only oxygen and silicon exist in greater quantities. It was only in 1808 that Sir Humphrey Davy, the British electro chemist, established the existence of aluminum (Cobden *et al, 1994*). The next ″discovery″ of aluminum was the purpose of its specific gravity by the German scientist Wöhler in 1845 (Cobden *et al, 1994*). He established one of aluminum's outstanding characteristics - lightness. He also discovered that aluminum was easy to shape, was unchanging in air, and could be melted with a blow burn down. Due to research from a blow torch melted aluminum shifted to France. But it cost him money to produce, making aluminum more precious than gold, silver or platinum at that time. Deville was subsequently able to produce aluminum at a cost of $37 per kg but that was still too high to launch the metal commercially. From 30 years later improvements in production methods made in association with Hamilton Y. Castner, an American chemist had lowered the price to $18 per kg. The total annual amount at this time was only 15 tones. Then two unknown young scientists - Paul Louis Toussaint Héroult of France and Charles Martin Hall of the United States took over the technical search for the low cost production of aluminum (Cobden *et al, 1994*). They worked individually, each uninformed of the others activities, in their particular countries. In 1886, after emotion breaking failures and little encouragement, the two scientists almost simultaneously approached with the same new process. They had the knowledge that if some substance could be found which would conduct electricity and in which aluminum oxide (Al_2O_3), known as alumina, would dissolve, and then an electric current passed through the solution could credit the aluminum as metal. There are some solutions which will dissolve aluminum, but these are water solutions. The oxygen combines with the carbon at the anodes and is given off as carbon dioxide gas. This became the first industrially applied method of making the metal aluminum from alumina, and is the one still in use today (Cobden *et al, 1994*).

One of the great challenges of this century is the high demand for lightweight metals with promising physical, chemical, and mechanical properties for various structural and functional applications. In lightweight metals family, aluminum is one of the most abundant lightweight metals in Earth and is used in many industries such as aerospace, automobile, and marine (Khan *et al, 2017*).

Pure aluminum is relatively soft and ductile and tends to follow to a cutting tool, forming a built up edge and long chips. It requires special machining techniques to avoid producing rough surfaces and heavy burrs. Pure Al with low strength and high ductility is less interesting for certain applications where high strength and lightweight are needed. Although alloying pure Al with other metals such as Cu and Zn would result in higher strength, there is a limit to how much these elements can be added. On the other hand, Al matrix composites can be compromise excellent properties to compete with high strength and high density metals (Cobden *et al, 1994*). Therefore, shall select Al matrix composite materials, i.e. Aluminum Titanium diboride (Al – TiB_2).

Titanium diboride (TiB_2) is an extremely hard ceramic which has excellent heat conductivity, oxidation stability and resistance to mechanical erosion. TiB_2 is also a reasonable electrical conductor, so it can be used as a cathode material in aluminum melting and can be shaped by electrical discharge machining. TiB_2 is very similar to Titanium carbide, an important base material for cermet's, and many of its properties (e.g. hardness, thermal conductivity, electrical conductivity and oxidation resistance) are superior to those of TiC. TiB_2 does not occur naturally in the earth.

The aim of this work is investigation of the formability characteristics effect on Al matrix composite material. Metals like aluminum that has been joined with a high percentage of other elements such as TiB_2. Formability is the ability of a given material work piece to undergo plastic deformation without being damaged. The plastic deformation capacity of materials, however, is limited to a certain extent at which point the material could experience fracture; thus its investigation is critical for successful processing of materials during bulk deformation. In this work investigated, it was undertaken to generate the formability of Al-TiB_2 composites for various percentage TiB_2 powder such as (0%, 4%, 8%, and 12%). The material properties such as strain hardening exponent and strength coefficient were determined using stage wise compression test to generate the formability limit diagram (*Desalegn et al, 2014)*. Forming limit diagram (FLD) is a valuable tool for analyzing the deformation mechanics of metal forming. It has been used as a reference to estimate how the material close to failure (*Desalegn et al, 2014).*

1.2 Problem statement

Most production factories have been facing a great challenges or problems due to the customer demand in lightweight and high strength material, especially used in aerospace, automotive, and marine industries. Therefore, it was essential developed and study lightweight with high strength composite material, i.e. Al-TiB_2. But, this material is sensitive, which may cause damage, cracking and tearing, especially in cold forming. Here of, this work study the formability of Al- TiB_2 to remove the problems by which the properties of the material i.e. deformation, strength, strain hardening exponent and strength coefficient were determined using stage wise compression test.

1.3 Objective of the study

1.3.1 General Objective

The general objective of this study is to investigate the formability behavior of Aluminum Titanium diboride composite material with various percentage compositions.

1.3.2 Specific objective

- To prepare Al-TiB_2 composite with various composition.
- To determine the formability of the Al-TiB_2 composite material with compression test.
- To examine the micro structural change using optical microscope technique for various composition i.e. 0%, 4%, 8%, and 12% TiB_2 of Al-TiB_2 composite material.
- To perform the finite element modeling or numerical simulation by using DEFORM software.

1.4 Scope of the study

The main focus of this thesis is investigation of the formability behavior of Al - TiB_2 composite material. The sample was prepared by with stir casting technology changing the percentage of Titanium diboride (TiB_2). And also has been done compression test by using universal testing machine and Optical microscope to analyze the micro structures of the composite material. Simulation, calculations, assumptions, and selections were made as a consideration of a proper and realistic design. Finally, there are many measures of formability quoted in the literature, but there is a gap on formability of Al-TiB_2 composite material development work seems to focus on an empirical product of the material structure analysis. This makes it very difficult to define how good microstructures, which perform well during forming operations, can be developing. The justification for the formability criteria is another feature of the present work.

1.5 Significance of the study

This investigative research could be important to address the issues behind the forming of the composite material. This work gets good formability for aluminum with TiB_2 composite material from the compression test and other experiments such micro structure analysis. And also to minimize weight of product material and increase strength or increase life time of product. Fatherly, when analysis and testing the Al-TiB_2 composite material could know Al-TiB_2 composite material micro structure and the properties of the material, and also to develop the technology transfer.

1.6 Limitation of the study

In this study was broad a few challenges regarding the proposed fabrication method which excellence study, or development in more detail, include the effect of stirrer and stirring speeds, it may be feasible to reduce particle fracture, further improve wetting, and minimize porosity through improved understanding of the process of mechanical stirring, during casting the melting temperature was not notable because of lake of electrical furnace, the microstructure and phase composition of the composite produced Variations in stirring and casting temperature can influence chemical reactions, and micro structure was not visible for with optical microscope used magnified to 20 micro meter.

1.7 Organization of the study

This thesis is organized in seven chapters. The first chapter includes introduction which provides back ground of the study, problem statement, objective, scope, significance of the study, and limitation of the whole research work. The second chapter covers the review of some journal articles, conference papers, which were referred during study. Also in relation and comparison with previse works, what is done in this study has been stated. The third chapter discussed about methods for completing specimen preparation, methodology of data analysis and testing activities. The applied methods, which are well-structured, provide a step by step approach to complete the task of this topic. Chapter four views about compression test result and micro structure result as well as numerical simulation are generalized or conclude how to change from pure Aluminum to its composite material which are add to different percentage composition of Titanium diboride powder. Finally, the last three chapters cover conclusions, recommendations and future work, references and appendix respectively.

CHAPTER TWO

2. LITERATURE REVIEW

2.1 Introduction

Conducting the literature review was done prior to undertaking the thesis. This will critically provide as much information as needed on the technologies available and methodologies used by other research counterparts around the world on the topic. This chapter provides the summary of the literature reviews on topics related to the formability behavior of Al-TiB_2 composite material.

2.2 Literatures view

2.2.1 Al-based composite materials

Jiwei Geng et al (2016) study to The Al-Cu-Mg alloy is one of the most commonly used aerospace Al alloys, which has been intensively developed recently in order to meet the future industry requirement. The particulate reinforced metal matrix composite is one of the developed materials with higher mechanical properties in comparison with the metallic counterpart. For example, the particulate reinforcements like SiC, B_4C, and Al_2O_3 particles have been widely investigated in the Al-Cu-Mg alloy composites. In these composites, the particles are usually added by ex-situ methods with the larger particle size in micron scale and higher particle volume fractions. The SiCp/Al composites are the typicalmaterials in this category. Recently, the in-situ TiB_2/Al alloy composites have been successfully prepared via the salt-metal reaction route, which showed the better and balanced mechanical properties. Nevertheless, TiB_2 particles are prone to coexist with the second phases (SPs) during solidification process.

Ahmad Changizi et al (2011) Metals like aluminum that has been combined with a high percentage of other elements such as TiB_2. In Aluminum matrix composites (AMCs), the ceramic reinforcements are generally oxides or carbides or borides such as Al_2O_3, TiB_2, TiO_2, SiC, TiC, B_4C, etc. The processes root of manufacturing, shape, size, and chemical affinity with matrix material of reinforcement materials influence their microstructure, physical properties, tribological properties and other desirable properties of the composite. The formation of strong chemical bonds at the interface is favorable for the wetting of reinforcement by molten metal, which is considered as an important aspect in MMC synthesis. The lower wettability adversely affects the properties of the composite. Non-wetting of the reinforcement with the molten metal is primarily caused by the presence of oxide films on the surface of molten metal and the adsorbed contaminant on the reinforcement. Metallic coatings on the reinforcements, addition of reactive elements, such as magnesium, calcium or titanium, to the molten metal and heat treatment of particles before addition are some of the techniques to improve metal–reinforcement wettability.

2.2.2 Based on properties of Al-TiB_2 composite materials

Poria S. et al (2016) this work deals to Analysis the properties of Al-TiB_2 Composite material. There are two parts in MMC. One is matrix phase and other one is reinforcement. As matrix, aluminum, magnesium, titanium alloys are mainly used. Among MMCs, aluminum (Al) based metal matrixes are more popular for usage as wear resistant components in automobile or components used in extremely abrasive, corrosive environment like chemical, aerospace industry. Actually in stir casting method, base metal is melted using some type of furnace and particles are mixed with the molten metal continuously with the help of mechanical stirrer. TiB_2 reinforced aluminum alloy MMCs exhibit better mechanical and tribological properties compared to other ceramic particulates reinforced aluminum MMC. Most important reason is TiB_2 does not react with molten aluminum which leads to no brittle reaction product in the interface. As well as TiB_2 holds excellent properties like high Young's Modulus (345-409 GPa), high Elastic Modulus, high hardness, low density, high wear resistance. TiB2 reinforced aluminum alloy MMCs are used as crucible in chemical industry, wear resistant parts in ceramic, aerospace industry. A model of wear prediction of stir cast Al-TiB2 composites using response surface methodology was proposed.

Roya Darabia et al (2017) study To Investigate the effect of material properties and arrangement of each layer on the formability of bimetallic sheets and with the effect of specimen thickness, stretching load. In this paper, an analytical model based on the M-K theory using Barlat-Lian and Hill's non-quadratic yield function was developed to study the formability of two-layer sheets. Experiments are also carried out on AL3105-St14 two-layer sheet to validate analytical model. Accordingly, the influence of material properties and arrangement of layers on the formability of two-layer sheet was investigated. The formability of two-layer sheet improves with increasing the values of strain hardening exponents (n_i) and the strain rate sensitivity coefficients (m_i) of its components. The most effect of these factors was observed in the plane strain condition on FLD0 values. Generally, the increasing of thickness of layers causes formability enhancement but higher thickness of low formable layer (aluminum) leads to a lower FLD0value in the plain strain condition. the arrangement of layers as $0^\circ-0^\circ$ in aligned rolling direction is recommended to reach better formability of two-layer sheet.

Tino Wollmanna et al (2018) study to perform the Stiffness properties and forming behavior of Thermoplastic fiber metal laminates by means of deep drawing and with its process parameters i.e. Blank holder force, punch force, punch size, corner radius and so on. Hat profiles with a clamping distance of 110 mm, width of 80 mm and height of 55 mm are fixed at the bottom edge and constrained to a vertical displacement as well as loaded with a force up to 35 N at the upper edge. As the tests are only performed in a linear-elastic region of the material, the spring stiffness can simply be calculated by dividing the applied force by the linear displacement of the upper edge. The spring stiffness of two different layups, which are subsequently explained, with 0.25 mm thick steel cover sheets were investigated within this work. With regard to the analytical approach presented, that a blank holder force of 100kN was not high enough to avoid intense wrinkling of the cover sheets in the flange as well as in the wall of the cup while almost no wrinkles could be observed at 200kN. At a Blank holder force of 300kN there was no wrinkling but a crack could be detected in the region of the punch corner radius. The presented experimental, analytical and numerical investigations of the forming behavior show a good accordance with one another, as well as a high potential for the design and development of carbon fiber-reinforced metal laminate components. Specifically, the formability of the presented material due to its thermoplastic matrix material allows short processing times which are important for an application in the automotive industry, as example.

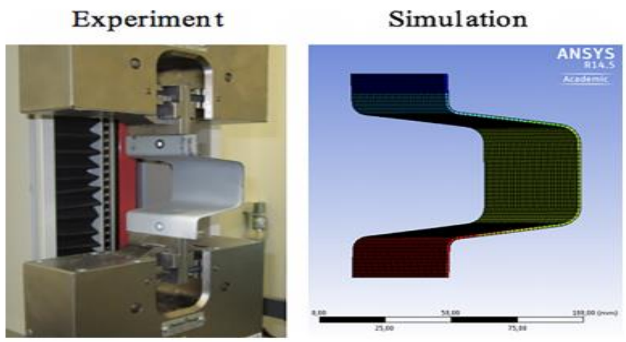

Figure 2. 1 Experimental and numerical setup for the determination of the spring stiffness *(Wollmanna et al, 2018)*

Hosamani G.G. et al (2016) works was to analyses Characterization of SiC reinforced aluminum matrix composites by using stir casting method. And their processing parameters were SiC percentage rate, melting temperature, cooling temperature, stirrer speed, compression load. First the pure solid Al was melted in furnace and when the temperature of the liquid Al reached around at 700-750^{o}C, SiC powder is added in molten Al metal. After that the powdered form of SiC was added and the liquid metal-reinforcement mixture was stirred for about 15-20 minutes at an rpm of 450-500. Lastly the composites were poured in preheated molds at 670^{o}C. The melt was allowed to solidify in the mold for about 4-5 hours so as to provide enough time for cooling and then the specimens were taken out. Compression test was performed using computerized universal compression testing machine. Specimens of each composition 3% and 7% SiC-Aluminum of dimension 10 mm sided cube was prepared for testing. Test method ASTM D 695 was referred. The results of the compression tests of 3% and 7% SiC- Aluminum is illustrated as Compressive strength (MPa) 332 and 380 of the AMCs increases with increasing SiC % composition. This is because SiC being strong material added to Aluminum which require high strength to compress the AMCs. Characterization of silicon carbide reinforced aluminum matrix composites by using stir casting method.

Figure 2. 2 Tensile test specimens *(Hosamani et al, 2016)*

2.2.3 Based on fabrication techniques of Al-based composite materials

Suresh S. et al (2013) Study process development in stir casting of TiB_2 on Al6061 MMC In the preparation process of this method, stirring has been carried out in graphite crucible in coal- fired furnace with continuous stirring of the molten metal- matrix gives homogeneous mixture of composites and instantaneously poured into the sand to get solidify. Coal is used as a fuel for preparation. The working diagram of the coal- fired furnace. Aluminum 6061 is used as the matrix material in the present investigation, and details of the composition. Aluminum Alloy (Al6061) was melted in a crucible by heating it in a blower furnace at 750°C for twenty minutes. The TiB_2 powder is preheated at 700oC. The furnace temperature was first raised above the liquid temperature of Aluminum near about 750oC to melt the Al6061completely and was then cooled down just below the liquid us to keep the slurry in semi-solid state. The stirring was carried out with the help of the drilling machine for about 10 minutes at stirring rate of 450 rpm. At this stage, the preheated TiB2 particles were added manually to the vortex. In the final mixing processes the furnace temperature was controlled within 700 ± 10oC. The mixture was poured into the mold cavity (size 150 × 15 × 15 mm) and allows this for cooling by keeping the mold in room temperature.

Animesh Talapatra et al (2014) works to find out the Erichsen number (EN) of unidirectional laminated polymer composite sheet materials and the usable parameters are temperature, sample thickness, and speed of spindle. The material was subjected to a shortterm heating to 200°C, causing softening and partial melting of the inner LDPE sheet and penetration of the polymer into the glass reinforcement. As cooling method, quenching was applied in order to eliminate negative effects of crystallized. From the experiment they concluded that more the Erichsen Index of a material more the stretching formability property of the material and is more suitable for general use than ones with lower index.

Davey S. et al (2012) works, to consolidated composite blanks of carbon fiber/polyether, with the process parameters that Temperature and press force combined composite blanks of carbon fiber/polyether ether ketone were stamped until failure with a hemispherical punch under various temperatures. Real-time strain measurements were extracted using three-dimensional photogrammetry. The apparatus in the experiment consisted of a hydraulic stamping press and a fan-forced Oven. The CF/PEEK and aluminum samples tested in this study were 180mm circular discs. During forming, the strain on the bottom surface of the blank was recorded using a strain measurement system manufactured. The results were evaluated with benchmarks used in metal forming. These were then compared to aluminum blanks formed under similar conditions. Under certain circumstances, the composite exhibited comparable formability to aluminum. This is particularly significant, as carbon fiber/polyether ether ketone is a high performance composite with superior specific mechanical properties compared to monolithic metal alloys. These results highlight the potential for composites such as this to replace heavier metals in various industries, without sacrificing performance or increasing manufacturing expenses. This work shows that the formability of carbon fiber/polyether ether ketone composite sheets in stamp forming processes is strongly dependent on the preheat temperature of the material. High temperatures allow for significant material flow at 45°to the fiber direction. This permits forming depths approaching those of 5005- H34 aluminum, and formed parts with a much higher specific strength.

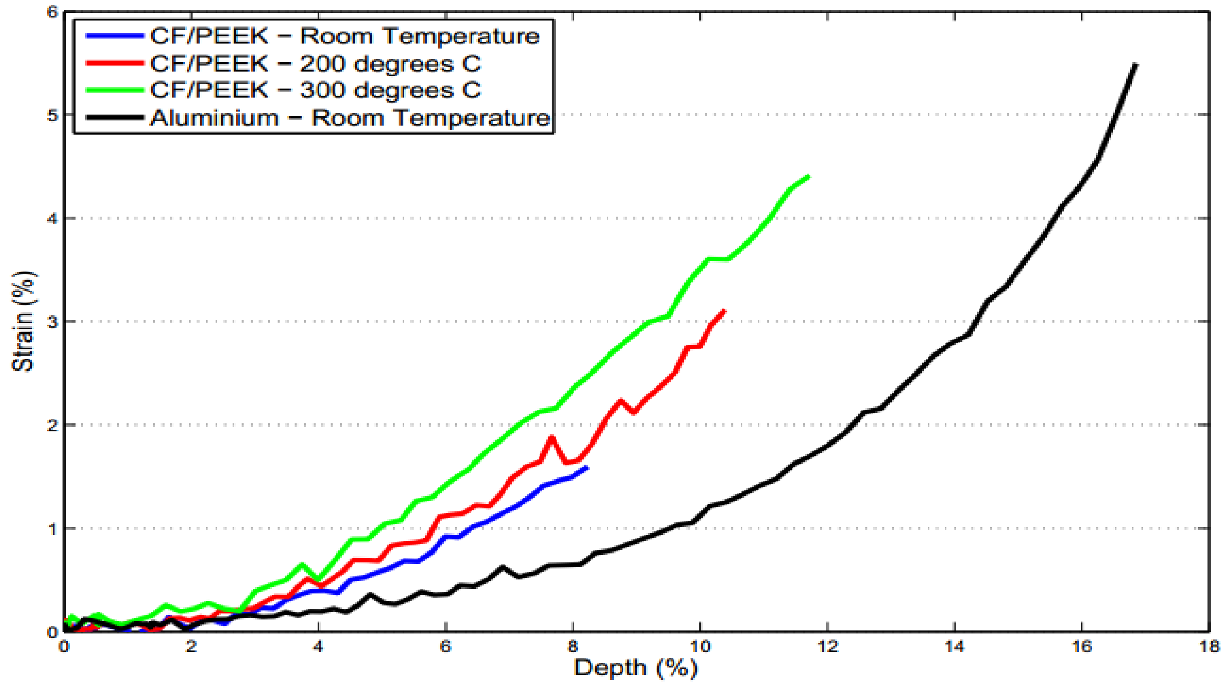

Figure 2. 3 Evolution of major strain at 45° to the fiber direction (rolling direction) of the material (*davey et al, 2012).*

Xiangrong Tian et al (2018) study to prepare and forming technology of particle reinforced Aluminum Matrix Composites and with their process parameters i. e Particle size, melting temperature, cooling temperature. The agitation method, also known as the whirlpool method, was the basic principle of adding the particle reinforcement directly into the molten aluminum alloy melt, through a certain way of mixing, so that the particles dispersed in the aluminum alloy melt, and finally into the PRAMCs melt. Squeeze Casting Due to the solidification of the composite under high pressure, it not only improves the wettability of the molten metal and the reinforcing particles, but also eliminates the defects such as loose and porosity, which greatly improves the strength and plasticity of the composites. Because the particle reinforced aluminum matrix composite material has good comprehensive performance, its specific strength is higher than the traditional aluminum alloy, and the modulus is even more than titanium alloy, used as high performance structural materials, can improve the structural safety, or optimize the structural design. At the same time, the particle reinforced aluminum matrix composite material excellent physical properties, in some special circumstances can be used as functional materials. The development prospect is very broad and will lead the revolution of advanced materials through large-scale production and application.

2.2.4 Based on formability behavior of Al-TiB_2 composite material

Paweł Hyjek et al (2015) study to Investigate deformation behavior of Al–SiC composite material consisting of AA6061 matrix with 15%SiC reinforced particles. They use the process parameter of High mixing temperature, strain rate, particle size 1 or 8 μm in diameter and the matrix alloy has been investigated. First mix the powder Al alloy and SiC particles with ultrasonic technique. After mixing hot welding vacuum at 823k for 1h temperature heated on heat transfer subjected to compression test by with uniaxial compression test machine. Based on the results of investigation the influence of the reinforcing particle diameter, temperature and strain rate on the values of flow stress was determined. The strain hardening is compared with estimates of the theoretical strength of 6061 aluminum alloy. The cooperation of the deformation and precipitation strengthening mechanisms with structural recovery, mainly dynamic recovery and recrystallization process has been also analyzed. Microstructural observations of surface relieves have been also conducted to correlate the mechanical characteristics with structure evolution. The investigations have proved the usefulness within limited range of temperature and strain rate of AA6061/SiC composites reinforced with 1 and 8 μm particles. The composite reinforced with 1 μm particles demonstrated higher (by a few percent) values of the yield point than the 8μm composite, which could be attributed to greater number of obstacles for the movement of dislocations. At higher temperatures, on the account of the occurrence of slip over the grain boundaries, the above-mentioned differences become less evident.

Desalegn Wogaso et al (2014) study to generate the forming limit diagrams for powder metallurgical aluminum–copper composites for different initial relative densities and copper contents. These process parameters are Compact pressure, melting temperature, density, and dimension of the specimen. The PM preforms were prepared from pure aluminum powder and aluminum–copper mix, and then The compacts were sintered in a muffle furnace at 550 ± 10^{o}C for holding period of 45 min. finally evaluate the deformation with ring compression test machine. Sintered aluminum–copper composite compacts of 2%, 4% and 6% copper content with different initial relative densities have been prepared by applying recommended powder compaction pressures. The material properties such as apparent strain hardening exponent and strength coefficient were determined using stage wise compression test to generate the formability limit diagram. The friction factor between tool and work piece interface are decreases with increase in the initial relative density for all the cases of copper content and increases with increase in the content of copper in the composite. With increase in the content of copper in the composite, the critical transition density values increases from 84% of pure aluminum to 85.3% with 2% copper addition, to 86% with 4% copper addition and 87.5% with 6% copper addition which narrow the safe working zone of the materials.

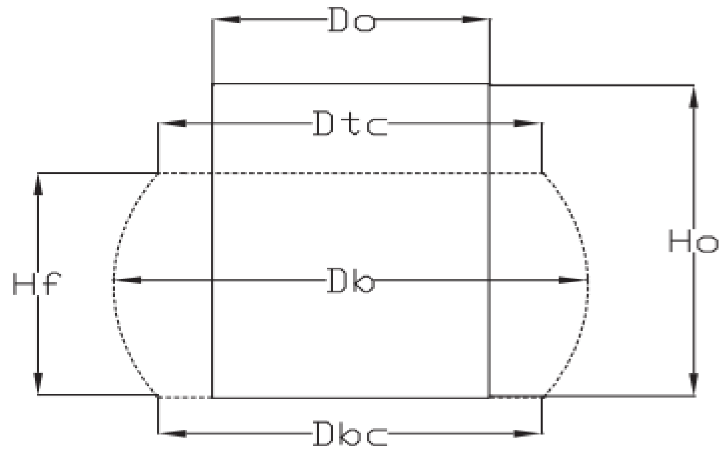

Figure 2.4 Upset forging test preform geometry before and after deformation (*Desalegn et al, 2014*).

Sumesh Narayan and Ananthanarayanan Rajeshkannan (2017) Studies on formability of sintered aluminum composites during hot deformation using strain hardening parameters are used to study the workability behavior or determining the failure zone. Hence, the amount of smaller and fine pores existing in Al-4TiC compact is higher compared to other materials tested here and hence, for the same reason the critical relative density is higher for TiC composite in comparison with other composites.

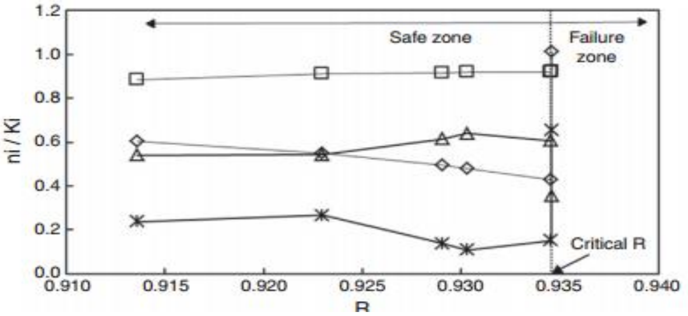

Figure 2.5 Workability limit diagram for PM Al4TiC composites (*Sumesh Narayan and Ananthanarayanan Rajeshkannan, 2017).*

Khan, M et al (2017) study to evaluate Cold formability of friction stir process aluminum composites by with bend ductility test. There process parameters are rotational speed, traverse speed, tilt angle. Aluminum plate was drilled for preparing cavities. For the combined reinforcement, MWCNTs and B_4C particles were introduced, finally, to evaluate cold formability by with different tests. Composites containing carbon fractured during bending while those containing boron carbide particles survived; hybrid composites showed cracking but less than those containing solely. Weak interfacial carbon/aluminum bonding and inadequate distribution were found to be the possible reasons. Al5083 surface composites were prepared by single pass Friction stir processing (FSP) containing both individually reinforced and combined multiwall carbon and boron carbide (B_4C) particles. The mechanical characterization of surface composites was performed by tensile, hardness and cold-formability tests. The composite containing B_4C particles showed ~ 12% and ~ 28% improvements in hardness and tensile strength compared to reference specimen, respectively. It also qualified the bend-ductility test without any surface cracking. The composite containing multiwall carbon showed ~ 50% decrease in fracture strain while hardness and tensile strength were comparable with reference specimen.

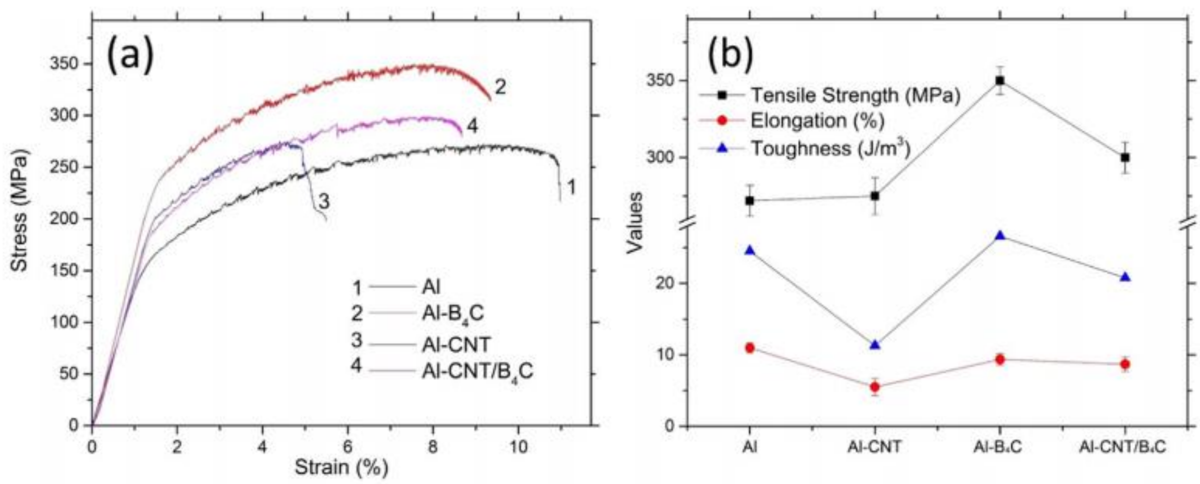

Figure 2.6 (a) tensile stress-strain curves, (b) tensile strength, fracture strain and toughness plots *(Khan, M et al, 2017).*

Lee M.S. et al (2016) study to assess (CFRP) on CR340 plates formability and potential use in vehicle parts, deep drawing tests were conducted for this hybrid composite material with various process parameters such as curing temperature, size of the blank, punch force, punch velocity, blank holding force, and laminating methods. The CFRP composites were fabricated using carbon fiber from Toray Industries Inc., and plain weave fabric. CR340 steel sheet was used to laminate the CFRP composites. Finally using deep drawing technique studded the formability of different size specimens. The forming depths decreased to 11.2, 10, and 8 mm as Bf increased to 15, 30, and 90 kN, respectively. In the case of the CR340/CFRP^{R*} composite material, the forming depths were 18, 13.5, and 8.5 mm, respectively. This indicates that CR340/CFRP^{R*} has much superior formability than the CR340/CFRP composite material. At Bf= 15 kN, the forming depth without fracture of the CR340/CFRP^{R*} composite material was 16mm, which is greater than that of the CR340/CFRP composite material(11 mm).

Bernhard Maron et al (2016) works on evaluate the forming processes of carbon fiber reinforced thermoplastic composite tubes by experimental and numerically using Finite Elements (FE) methods. And there process parameters are temperature, pressure, and velocity. Braided hoses were used to manufacture flat specimens. The plates were consolidated in the autoclave at 240^{o}C and a pressure of 5bar. The specimens are clamped emulating the pipe forming process conditions in 458 direction and are drawn through the heated metal plates at a normal pressure of 50 kPa and sliding velocities of 0.1, 0.5 and 1 m/min. The numerical results (a_{exp}, b_{exp}) are adjusted to the initial experimental level FS (a1, a2, b1, b2). For both cone angles, the numerical parameter K=1 (a1, b1) represents the trend of a rising force during forming well. However, in case of configuration b1 the force level is overestimated. In contrast, with K=0.01 (a2, b2) a reliable estimation of forming forces cannot be achieved.

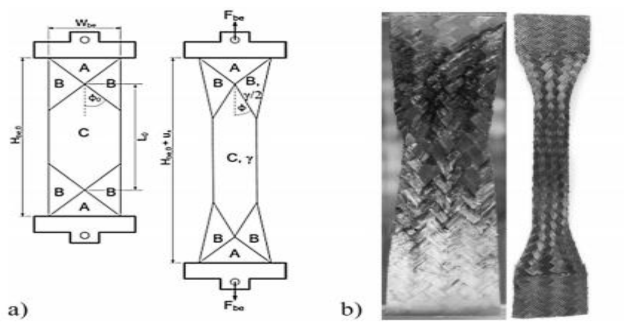

Figure 2.7 Bias-Extension-Test: (a) Characteristic shear zones, (b) deformed test specimen for different test temperatures *(Maron et al, 2017)*

Jufu Jiang, Gang Chen, Ying Wang (2016) study to investigate the compression mechanical behavior of 7075 aluminum matrix composite reinforced with nano-sized SiC in semisolid state. By with the process parameters i.e. melting and cooling temperature, sample size, punch force the 7075 aluminum alloy was melt at 650 °C and SiC added into the molten and treated by a 2-kW ultrasonic device for 20 min. after stirred was solidified the sample. Three stages such as rapid increase of true stress decrease of true stress and steady state by with Isothermal temperature and soaking time influence. The compression velocity when decreases from 5 mm/min to 1.5 mm/min, the steady stress decreases significantly. It indicates that semisolid compression deformation is sensitive to deformation velocity (i.e. compression velocity). Compression velocity affects slightly on the change of macro appearance of the sample.

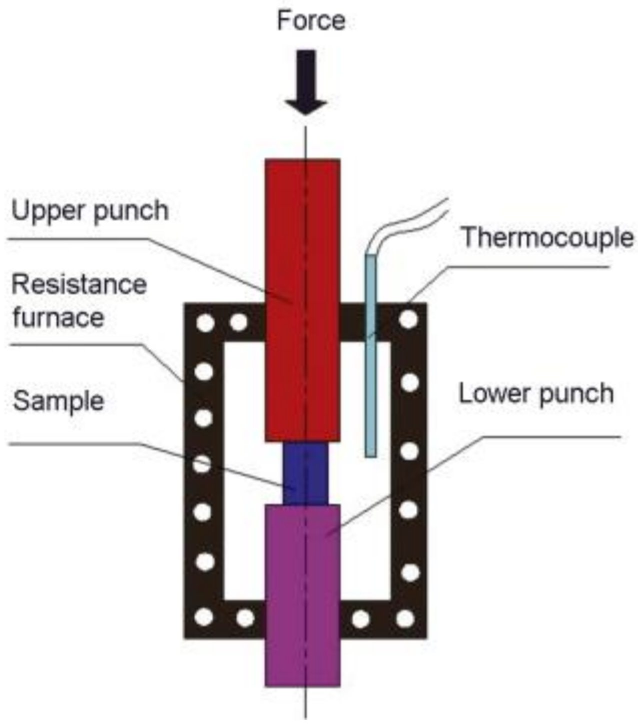

Figure 2.8 semisolid compression experimental devices *(Jufu Jiang, Gang Chen, Ying Wang, 2016)*

Wentian Wang et al (2015) study to investigate the forming limits of a flax fiber reinforced polypropylene composite through stretch forming experiments by use the process parameters i.e. Fiber density, thickness, etc. The major mechanism in failure of this class of material systems is the low elongation-to-failure behavior of the fibers, and hence a criterion based on the fiber strain is used in this work. Both the new FLC and the Maximum Strain failure criterion have been successfully implemented in FEA simulations. And also the $45^o/45^o$ specimens can exhibit a larger failure depth compared to $0^o/90^o$ equivalent specimens, shear deformation can aid in superior formability (failure depth) for the composite.

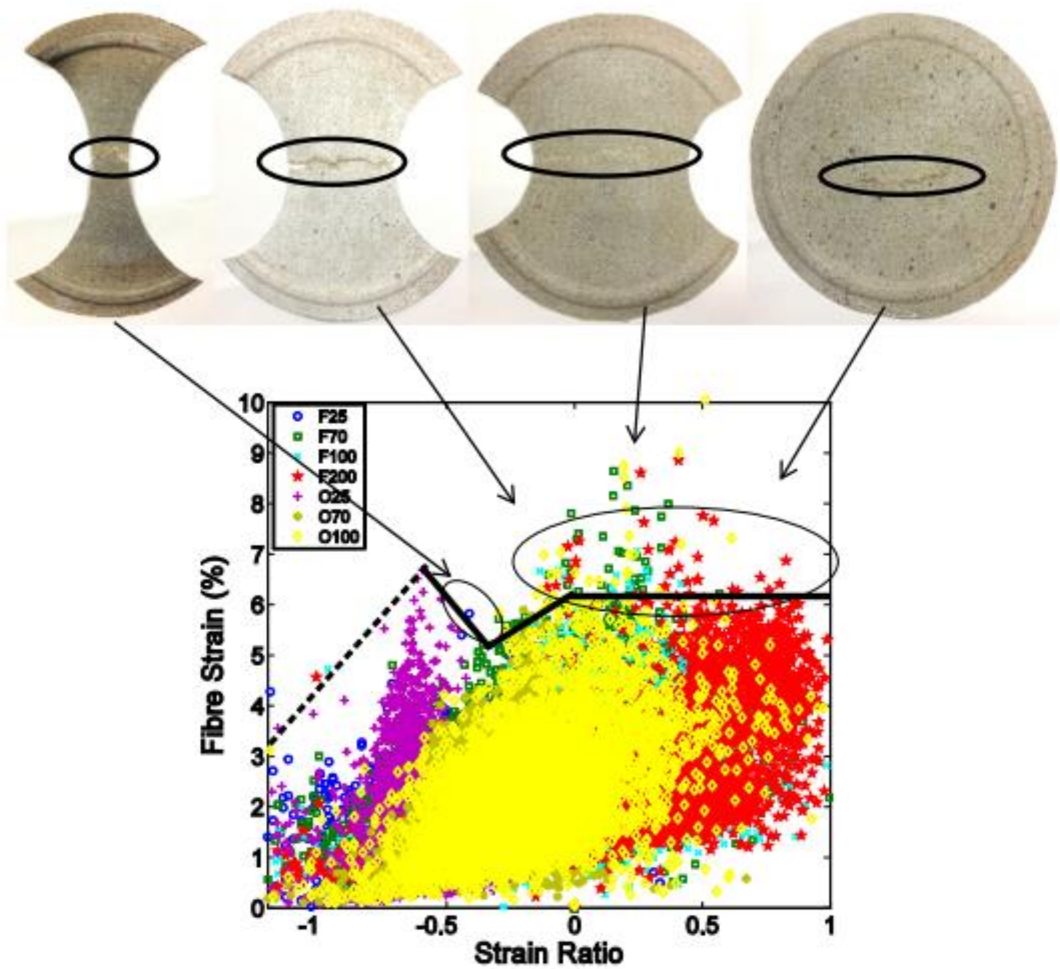

Figure 2.9 the new FLC over the surface strain distributions of all specimens at the stage of failure *(Wang et al, 2015)*

Hyun-Joon Juna et al (2009) study was to perform the Effect of crystalline phases on deformation and warm formability of a bulk metallic glass composite within super cooled liquid region. And the process parameters are melting temperature, transition temperature, crystallization onset temperature, strain rates and punch force. After specimen preparation for with fabricated by an injection casting a series of compression tests have consequently been performed using the specimens with 2 mm and 3 mm diameters. Extrusion tests were also carried out for the specimens with punch jig force. The viscosity of glassy matrix increases rapidly above the volume fraction of crystalline phase approximately 40% from the Einstein–Roscoe relationship. The formability of this BMGC within the SLR was thus found to be quite poor due to the large volume fraction of dendrites, which hinder the viscous flow of glassy matrix.

Atturan U. et al (2017) works to determine the deformation behavior of TiB_2 reinforced A357 aluminum alloy composite foams under compressive and impact loading. With understanding the process parameters are melting temperature, cooling temperature, density of foam, equivalent diameter, and aspect ratio, circularity of cells, impact velocity, and impact load. After melting the foam and stirring Cooling of the foam was carried out by allowing Pressurized air at constant flow rate. Optical and scanning electron microscopic studies were carried out on both cell walls of foam before and after compression testing. Drop weight impact tests were carried out on foams with relative density varying from 0.1 to 0.45 at a velocity of 10 m/s. Plateau stress values of A357-xTiB2in-situ composite foams under compression loading of 5TiB2foams exhibit plateau stress values slightly greater than 10TiB2foam. Energy absorbed by the 5TiB2foams during compression is greater than $10TiB_2$ foams. The gas-metal interface and thick inter dendritic region which are brittle in nature made the $10TiB_2$ foam inferior to 5TiB2foam. The energy absorption is insensitive to a displacement rate of 1.6×10^{-5} m/s (compression) to a rate of 10 m/s (impact).

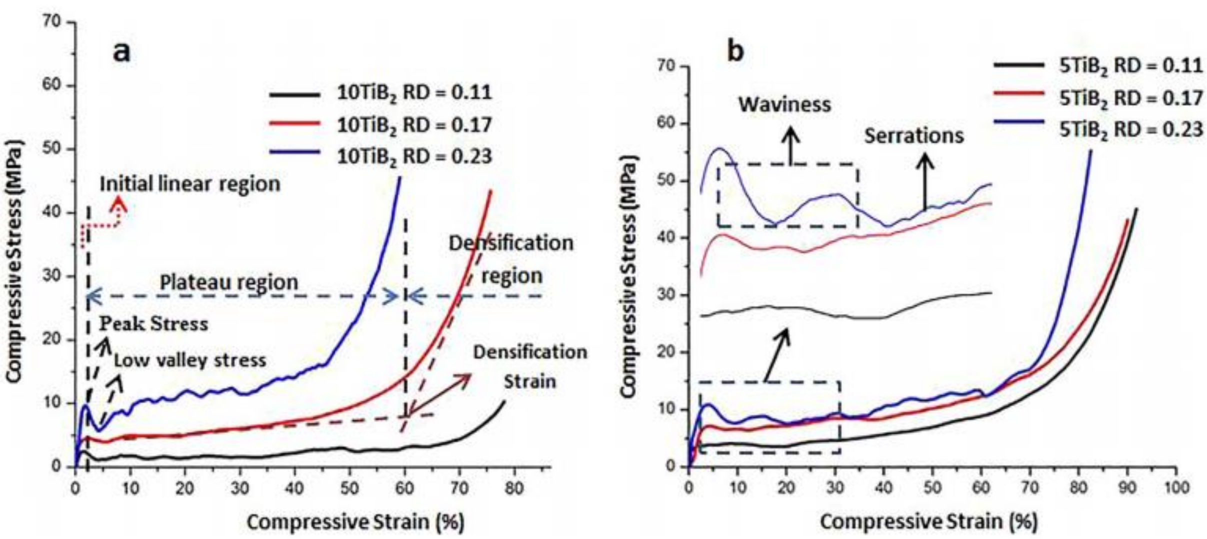

Figure 2.10 (a) Compression stress-strain plots of $10TiB_2$ and (b) $5TiB_2$ foams with 3 different relative densities *(Atturan et al, 2017)*

Farbod Nosrat Nezami, Thomas Gereke, Chokri Cherif (2017) works on manipulate the forming of composite reinforcements for the suppression of forming defects and with the parameters are targeted stress, specimen size. A geometrical rework of the design or further optimization of the material guiding strategies must be carried out, or an alternative textile should be selected. a significant increase in quality, exemplified by the reduction of wrinkle formation and the waviness of the fibers, is apparent. For the first time, the influencing of the draping behavior of a single fabric during full-stack forming has been demonstrated. The new approach is highly suited for an automated preforming process with low cycle time.

Meyer B.C., Ch.V. Katsiropoulos, Sp.G. Pantelakis (2009) works was to investigate the hot forming behavior of non-crimp fabric peek/c thermoplastic composites. The quality of the stiffeners produced using the hot forming process has been assessed with regard to surface appearance and internal defects using optical microscopy and C-Scan analysis. Although the APC-2/AS4 still provides in average a better quality, the use of the NCF composites led also to competitive products. The comparison has shown that the hot forming process may be used for the cost effective production of simple geometry parts from thermoplastic NCF composites providing an acceptable quality. The drape ability tests exhibit an excellent formability of three out of four thermoplastic NCF allowing the direct lay-up in a curved form before consolidation. Further systematic investigation and a material optimization are needed to improve the consolidation quality and reduce porosity of the more drape able thermoplastic NCF products, i.e. the NCF1 and NCF2 (commingled) as well as the NCF3 (fleece). The NCF-4 variant in its current form exhibits the best internal quality and has demonstrated comparable or even better mechanical properties than the reference. It could be used to save lay-up time for simple flat parts in current manufacturing processes.

Hengcheng Liao et al (2015) study is to determine hot deformation behavior and processing map of Al–Si–Mg alloys. containing different amount of silicon based on Gleebe-3500 hot compression simulation. The process parameters are SiC percentage rate, melting temperature, cooling temperature, stirrer speed, compression load. The studied alloys were melted in the graphite crucible of 3 kg capacity, using an electrical resistance furnace. The melt was held at 760^{o}C for at least 30 min. After cooled to 720^{o}C, the melt was first degassed using C_2Cl_6 (0.06 wt.%), then added with Al–10 wt.%Sr master alloys and finally with magnesium ingot. Prior to pouring, the melt was held at 720°C for at least half an hour. After processed, it was cast in a cylinder iron mold with an inner diameter of 60 mm (preheated at 200°C). For isothermal compression test, small cylindrical specimens with 15 mm in height and 10 mm in diameter were cut from the cylinder castings, which were solution zed at 535°C for 6 h and then water-quenched in water. Due to impeding dislocation motion by a great amount of silicon particles, both S2 and S3 alloys have much higher state steady flow stress and deformation activation energy Q than S1 alloy. The differences in σ and Q between S2 and S3 alloys are thought to be due to the difference of recrystallization maturity during hot deformation. Based on the constructed processing maps, the instability domain area of S2 alloy with 7 wt.% Si is the largest among the studied alloys at the same strain. Due to much larger mushy zone of S2 alloy during solidification, the pore defects are prone to form in it that induces instability during hot deformation. It is also found that the strain has no considerable influence on the peak power dissipation efficiency during hot compression, but the effect of silicon content on it is not ignorable. In S_2 and S_3 alloys with high Si content, the peak power dissipation efficiency is less than that in S_1 alloy, meaning that S_2 and S_3 alloys are more difficult to hot deformation than S_1 alloy.

Hu H.E., Xin-yun Wang and Lei Deng (2013) study to investigate High temperature deformation behavior and optimal hot processing parameters of Al–Si eutectic alloy. Compression specimens with a diameter of 8 mm and a height of 12 mm were machined with the compression axis parallel to the extrusion direction. Compression tests were conducted to a predetermined strain of 0.69 on a thermal–mechanical simulator (Zwick/Roell 20) at 563, 603, 643, 683, 723 and 763 K and the strain rates of 0.001, 0.01, 0.05 and1s^{-1}, respectively. Generally, the deformation temperatures of Al–Si eutectic alloy during hot deformation is lower than that of the solidus temperature of the equilibrium phase diagram of Al–Si binary alloy exceeds 70 K to avoid the effect of partial melting on hot deformation. Deformation activation energy of the Al–Si eutectic alloy decreases from the maximum value of 178 kJ/mol at the strain of 0.1 with increasing strain when the strain is smaller than 0.4. Then the effect of strain on deformation activation energy (163–164 kJ/mol) of the alloy is negligible at higher strain than 0.4. The main high temperature deformation mechanism of the Al–Si eutectic alloy is dislocation movement. Higher deformation activation energy of 178 kJ/mol than self-diffusion activation energy of pure aluminum (142 kJ/mol) results from rupture of eutectic silicon crystals in the Al–Si eutectic alloy. The optimal hot processing parameters of the Al–Si eutectic alloy are deformation temperature ranging from 660 K to723 K, lower strain rate than 10^{-1}.5s $^{-1}$ and strain of 0.51–1.20.

Xiaopu Li et al (2016) study to determine the deformation behavior of Aluminum matrix composite materials by used uniaxial compression test that is SiC/AA6061 composites with different SiC volume fractions (5%, 10%, 15% and 20%) were fabricated by spark plasma sintering. By with the process parameters for milling speed, compact pressure, and sintering temperature the deformation behavior of the composites was studied by uniaxial compression test at temperatures from 573 K to 773 K and strain rates between 0.001 s^{-1} and 1 s^{-1}. Results indicate that the flow stress of SiC/AA6061 composites increases with the increase of SiC volume fraction, with the decrease of deformation temperature and with the decrease of strain rate. The main deformation mechanism of the composites is dynamic recrystallization, and the dynamic recrystallization degree depends on the processing parameters of deformation. Higher SiC volume fraction, higher deformation temperature and lower deformation strain rate promote the occurrence of dynamic recrystallization. The strain rate sensitivity and deformation activation energy of SiC/AA6061 composites are calculated. Results show that with the increase in deformation temperature and the decrease in SiC volume fraction, the strain rate sensitivity of the composites increases. From 573K to 773K, the average deformation activation energy of 5vol.% SiC/AA6061, 10vol.% SiC/AA6061, 15vol.% SiC/AA6061 and 20vol.% SiC/AA6061 are 207.91, 230.88, 237.7 and 249.87 kJ mol^{-1} , respectively. The optimum hot working zone of the SiC/AA6061 composites is in the temperature range of 723K to 773K at strain rates from 0.1 s^{-1} to $1s^{-1}$.

2.2.5 Based on applications of Al-TiB_2 composite materials

Pradeep Kumar G.S. et al (2016) study Aluminum alloys are being used extensively for various engineering applications due to its superior strength to weight ratio. Al-TiB_2 in application area have dimensional stability, excellent structural rigidity and a low thermal expansion coefficient, its excellent formability allows easier usage for secondary processes such as hot extrusion, rolling and forging. Aluminum based particulate reinforced metal matrix composites are widely used in automobile, aerospace, transport and marine industries owing to their exclusive properties like low density, light weight, high elastic modulus, improved strength and good wear resistance, when compared to unreinforced alloys.

Himanshu Kala et al. (2014) the growing requirement for advanced materials in the areas of aerospace and automotive industries had led to a rapid development of MMC's. In AMC the matrix phase is of pure aluminum or an alloy of it and the reinforcement used is a non-metallic ceramic such as SiC, Al_2O_3, SiO_2, B_4C, and Al-N. Aluminum alloys are more and more used due to good corrosion resistance, high damping capacity, low density and good electrical and thermal conductivities. AMC's have been tested and proved useful in different engineering sectors including functional and structural applications because of variation in mechanical properties depending upon the proportion of reinforcement and chemical composition of Al matrix.

2.3 Gaps in the literature

All of the above literatures are generally, as we have seen study related to the formability behavior of aluminum matrix composite material i.e. deformation, microstructure, failure and, other mechanical behavior of different Al alloy with different ceramic material and different alloys. Such composite materials are aluminum with as a matrix material and SiC, Cu powder, TiC, TiB_2, B_4C, Carbon fiber, metallic glass, bimetallic sheet, thermoplastic, SiMg alloy and Si alloy with as the reinforcements but not TiB_2.

Titanium diboride (TiB_2) is an extremely hard ceramic which has excellent heat conductivity, oxidation stability and resistance to mechanical erosion. TiB_2 is also a reasonable electrical conductor, so it can be used as a cathode material in aluminum manufacturing and can be shaped by electrical discharge machining. TiB_2 is very similar to titanium carbide, an important base material, and many of its properties (e.g. hardness, thermal conductivity, electrical conductivity and oxidation resistance) are superior to those of TiC. Therefore, to decide use pure aluminum and various percentages of TiB_2 had taken composite material mixed by with stir casting. And study formability behavior of this material and also analysis its micro structure. Generally, this work was not done others on this way.

CHAPTER THREE

3. MATERIALS AND METHODOLOGY OF THE WORK

3.1 Introduction

This chapter consists of methods for completing specimen preparation, methodology of data analysis and testing activities. The applied methods, which are well-structured, provide a step by step approach to complete the task of this topic. Based on these methodologies, there are three advantages expected. Firstly, the decision processes is completely made, reducing the possibility of moving forward with unsupported decisions. Secondly, by acting as check list of the key steps in a development activity and ensure that the important issues are not forgotten. Thirdly, these structured methods are largely self-documenting; in the process of executing the method, the record of the decision making process can be used for future reference.

3.2 Process variables considered in this work

The process parameter of these work are listed as follows

1. Percentage composition of TiB_2

Due to mixing the composite material that is pure Al- TiB_2 with (0%, 4%, 8%, and 12%) TiB_2 composition is to get different material properties of its composite.

2. Melting temperature

The melting point of aluminum is sensitive to purity, e.g. for 99.99% pure aluminum at atmospheric pressure it is 660^{o}C but this reduces to 635^{o}C for 99.5% commercial pure aluminum. And TiB_2 melts congruently at 3225^{o}C. The characteristics of high melting point and stability of TiB_2 make it suitable for high temperature structural applications. But we can take 800^{o}C to use properly mixing the molten metal and ceramic powder.

3. Stirrer speed
4. Compression load
5. Density of Material

3.3 Materials

For this study TiB_2 powder was selected as the reinforcement since it is an extremely hard ceramic and pure Aluminum that is Al1350 purity 99.5% ingot as matrix material. TiB_2 powder was mechanically mixed at solid state for taking 30 minutes. An electrical resistance furnace was used to melt the Al ingot, after melt add TiB_2 powder to get Al- TiB_2 composite material with the method of stir casting.

Table 3. 1 properties of Al 1350 (pure Al) and TiB_2

Properties	**Al1350**	**TiB_2**
Elastic modulus(GPa)	68.9	560
Density(g/c^3)	2.71	4.52
Poisson's ratio	0.33	0.14
Hardness(Kg/mm^2)	23	2600
Shear strength(MPa)	82.7	-
Tensile strength(Mpa)	55.2	339
Yield strength(Mpa)	267	-
Melting temperature (^{o}C)	660	3225

a.  b. 

Figure 3. 1 raw materials: a. Al ingot and b. TiB_2 powder

3.4 Fabrication techniques of Al-TiB_2 composite specimens

Al-TiB_2 composite specimens were fabricated by stir casting process. In this stir casting, ingots were placed inside the cavity of the Furnace. Then, Al ingots melt with its melting temperature 667$^o{}_C$ in electric resistance furnace. Hence, the mixed powders were added to the melt surface and mechanically stirring Titanium diboride (TiB_2) powder and Al molten metal with stir mixing blade for 5minites and 200rpm stirrer speed. The mixture was poured into a mold structure and cooled at room temperature. This procedure will repeat for various weight percentages (0%, 4%, 8%, and 12%) of TiB_2 and altogether four different composites are going prepare with four different weight composition of TiB_2.

Figure 3. 2 Specimen fabrication by stir casting process

The experimental program was designed to study the size and shape effect on compressive tests achieved on high-strength specimens. With these intentions in mind, choose the specimens sketched in the following figure 3.2. We can use cylinders and cubes of different sizes: the dimensions of the cylinders are 20 by 60, 50 by 150 and 100 by 200mm (diameter and height); the edges of the cubes are may be 33, 50, 67 and 100mm.

Long samples are disposed to buckling therefore the length of the specimen must be limited. And using small sample results and using large sample requires testing machines with large capacities. Cylindrical specimens are preferred to ensure uniform distribution of stresses; there are three types of specimens used, L ≤ 10D to avoid buckling.

1. Long specimens L = 8-10D to install deformation measurement devices for obtaining the stress strain curves and other mechanical properties like the Modulus of Elasticity, Resilience, Toughness, etc.
2. Medium specimens L = 3D to obtain compression strength of materials.
3. Short specimens L = 0.9D to test metals used as bearings since the friction induced in testing will resemble bearing conditions

According to the above three dimension standards medium size specimens was selected to this work to analysis compression test, but the test depends on the UTM machine that is L = 1.5D. As shown in figure 3.2 the sample diameter (D) is 20mm and height or length (L) = 30mm.

Figure 3.3 sample preparation for Compression test

Figure 3.4 Sample for microstructure investigations

The specimen is prepared by considering various process parameters and all the steps for the preparation of Al-TiB_2 composites are followed. The steps include Weight Calculation, Fabrication (Casting and machining) and Experiment conduct.

Table 3.2 aluminum 1350 composition

Element	Composition in %	
	minimum	maximum
Al	99.5	-
Si	-	0.1
Fe	-	0.25
Cu	-	0.02
Mn	-	0.01
Mg	-	0.02
Zn	-	0.03
Ti	-	0.02
Cr	-	0.01
Na	-	0.01
B	-	0.02
V	-	0.02
Ga	-	0.03
Others	-	0.02
Total	99.5	0.5

3.5 Mechanical testing

Mainly, this work studied and analyzed under formability experiment, must study compression test to generate the forming limit of the material and view stress-strain curve. It has been used as a reference to estimate how the material close to failure. The compression strength will estimate using a computerized universal testing machine. Compression of the base matrix pure aluminum and the developed composites (Al-TiB_2) at room temperature determined used universal testing machine. For uniaxial tests, the displacement is typically held at a constant rate, and displacement and resulting load are recorded. The load is measured by a series of strain gages, or "load cell," while the displacement can be recorded as displacement of the crosshead, or the beam on which the specimen load frame is mounted. For more precise load measurements, strain gages or an extensometer can be directly fixed to the specimen. To make direct comparisons between materials, loading responses must be normalized against sample geometry. Therefore, the dimensions of each sample are noted to compute stress and strain from load and displacement, respectively. Engineering strain can be calculated as:

$$\varepsilon = \Delta L/Lo$$

Where ΔL is the measured displacement and Lo is initial sample length along a single axis. Engineering stress can be calculated as:

$$\sigma = P/A$$

Where, ‘P’ is the applied load and ‘A’ is the cross sectional area of the sample normal to the loading direction.

In compressive tests, specimens are typically cylinders. With the sample geometry, a stress-strain curve can then be generated from the recorded load and displacement.

This section of the laboratory experiment involved subjecting Aluminum 1350 and its composite (different percentage composition Al-TiB_2) material to compression using the UTM servo machine. The samples were then placed between the compression dies to start compression testing. To measure the strains of the samples within the compression range, the samples were loaded with the load measurement directly attached to it. The samples were then unloaded, had the extensometer removed, and then compressed again then measure the displacement reap it again up to fracture.

Microstructural investigation was used the minimal level of porosity and showing micro structure of the composite material to compered matrix material that is pure aluminum founded in the optical micrographs.

The even distribution of reinforcement particles is a prerequisite in enhancing the mechanical properties of a composite. In addition studded the finite element simulation or numerical simulation by used DEFORMS software analysis.

3.6 Mathematical and Theoretical Analysis

Fracture is the separation, or fragmentation, of a solid body into two or more parts under the action of stress. The process of fracture can be considered to be made up of two components, crack initiation and crack propagation. Fractures can be classified into two general categories, ductile fracture and brittle fracture. A ductile fracture is characterized by appreciable plastic deformation prior and during the propagation of the crack. An appreciable amount of gross deformation is usually present at the fracture surfaces. Brittle fracture in metals is characterized by a rapid rate of crack propagation, with no gross deformation and very little micro deformation. It is similar to cleavage in ionic crystals. The tendency for brittle fracture is increased with decreasing temperature, increasing strain rate, and tri axial stress conditions (usually produced by a notch). Brittle fracture is to be avoided at all cost, because it occurs without warning and usually produces disastrous consequences. Fracture occurs in characteristic ways, depending on the state of stress, the rate of application of stress, and the temperature.

3.6.1 Analysis of stress

The compression of a cylinder sample between two flat dies represents the simplest type of pressing operation. Although at first glance this appears to be a simple type of experiment which is subject to easy analysis, in actuality a compression experiment is usually complicated by the presence of friction between the dies and the specimen. In the absence of friction, i.e., when the dies are very well lubricated, the uniaxial compressive force required to produce yielding is

$P_z = \sigma_o A$ (Beer et al, 2013)

$P_z = 276 N/mm^2 \times 314.16 mm^2$

$P_z = 86.71 kN$

The compressive stress σ induced by a uniaxial force P is given by

$$\sigma = \frac{4P_z h}{\pi D_o^2 h_o} \text{ (Beer et al, 2013)}$$

Where h = height of cylindrical sample at any instant during compression

h_o = original height of cylinder

D_o = original diameter of cylinder

But we can get the compression stress, compression strain, fracture point and true stress - strain curve in experimentally by with UTM compression test. The true stress-strain curve is called as Flow curve and the equation that describes the curve is called Flow equation. Generally the flow equations are empirical, fit equations. For Hollomon's equation, $\sigma = K\varepsilon^n$ where 'σ' is the true stress for particular true strain (ε), 'K' is the strength coefficient, 'n' is the strain hardening exponent is a flow equation. It should be noted that this equation is valid from onset of plastic deformation to maximum load at which necking starts.

ln (σ) = lnK + n(lnε) => Y = C + mX Plot graph between ln (σ) and ln (ε), n = Δ(lnσ)/Δ (lnε) and K = Δσ/Δε.

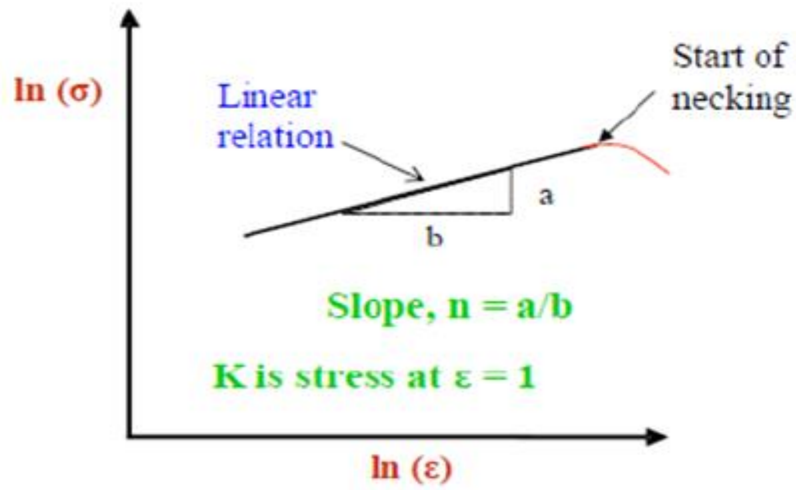

Figure 3.5 stress strain curve relation to solve 'K' and 'n' value *(Hollomon et al, 2008)*

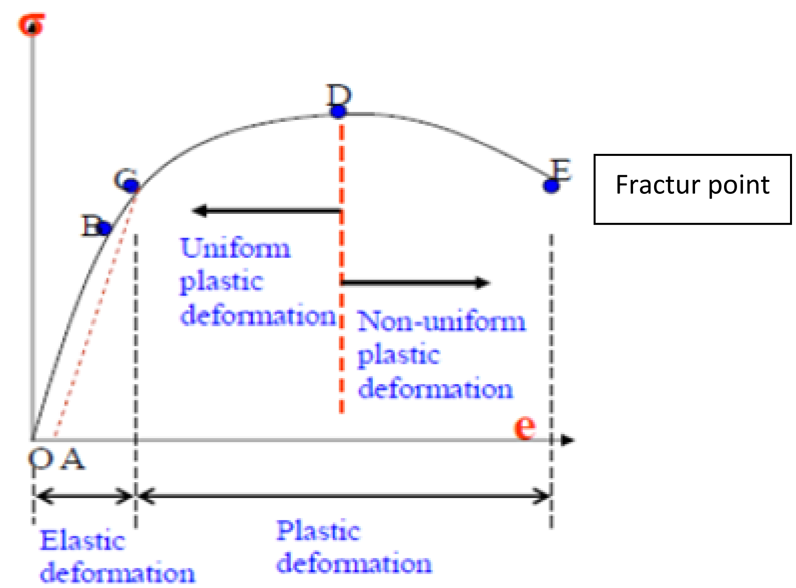

Figure 3.6 stress strain curve deformation analysis *(Hollomon et al, 2008)*

Strain hardening after yield point, further plastic deformation requires an increasing load but at decreasing rate. Work hardening strengthens the material, but at the same time area of cross-section is decreasing. The combined effect of these two phenomenon results in typical load progression curve. Necking–a local constriction begins along the gage section. From this point, incompatibility between strain hardening and area decrease arises. As a result, the load required for further progression decreases. This means that load carrying capacity of the sample decreases. After this, practically all plastic deformation is concentrated in the small necked region. Finally failure occurs in the necked region.

Table 3.3 Pure Aluminum sample dimension and its stress value Obtained by compression

Load (KN)	**D_o**	**D**	**h_o**	**h**	**Δh**	**σ**
0	20mm	20mm	30mm	30mm	0mm	0N/mm^2
20	20mm	20.85mm	30mm	28mm	2.00mm	58.58N/mm^2
40	20mm	21.05mm	30mm	23.5mm	6.50mm	114.94N/mm^2
60	20mm	21.84mm	30mm	20.04mm	9.96mm	160.16N/mm^2
80	20mm	22.00mm	30mm	18.6mm	11.4mm	210.45N/mm^2
100	20mm	25.23mm	30mm	16.3mm	13.7mm	200N/mm^2
120	20mm	28.36mm	30mm	15mm	15mm	189.97N/mm^2

Table 3.4 Al- 4%TiB_2 sample dimension and its stress value Obtained by compression

Load (kN)	**D_o**	**D**	**h_o**	**h**	**Δh**	**σ**
0	20mm	20.00mm	30mm	30.00mm	0.00mm	0.00N/mm^2
20	20mm	20.65mm	30mm	28.20mm	1.80mm	59.72N/mm^2
40	20mm	20.97mm	30mm	23.8mm	6.20mm	115.82N/mm^2
60	20mm	21.42mm	30mm	20.12mm	9.88mm	166.50N/mm^2
80	20mm	21.70mm	30mm	18.93mm	11.07mm	216.31N/mm^2
100	20mm	24.4mm	30mm	16.81mm	13.79mm	213.86N/mm^2
120	20mm	27.35mm	30mm	15.70mm	14.30mm	204.26N/mm^2

Table 3.5 Al- 8%TiB_2 sample dimension and its stress value obtained by compression

Load (KN)	D_o	D	h_o	h	Δh	σ
0	20mm	20.00mm	30mm	30.00mm	0.00mm	0.00N/mm^2
20	20mm	20.61mm	30mm	28.31mm	1.69mm	59.95N/mm^2
40	20mm	21.89mm	30mm	24.05mm	5.95mm	116.71N/mm^2
60	20mm	21.31mm	30mm	20.40mm	9.60mm	168.07N/mm^2
80	20mm	21.40mm	30mm	19.05mm	10.95mm	222.42N/mm^2
100	20mm	24.10mm	30mm	117.01mm	12.99mm	219.22N/mm^2
120	20mm	26.86mm	30mm	16.00mm	14.00mm	211.78N/mm^2

Table 3.6 Al- 12%TiB_2 sample dimension and its stress value obtained by compression

Load (KN)	D_o	D	h_o	h	Δh	σ
0	20mm	20.00mm	30mm	30.00mm	0.00mm	0.00N/mm^2
20	20mm	20.54mm	30mm	28.40mm	1.60mm	60.36N/mm^2
40	20mm	20.74mm	30mm	24.52mm	5.48mm	118.40N/mm^2
60	20mm	20.89mm	30mm	20.81mm	9.19mm	175.06N/mm^2
80	20mm	21.05mm	30mm	19.40mm	10.60mm	229.88N/mm^2
100	20mm	23.80mm	30mm	17.32mm	12.68mm	224.78N/mm^2
120	20mm	26.45mm	30mm	16.40mm	13.60mm	219.22N/mm^2

3.6.2 Analysis of Strains

Concept of strain: if a sample is subjected to a direct load, and hence a stress the sample will change in length. If the sample has an original length L and changes by an amount ΔL, the strain produce is defined as follows: strain = $\frac{\text{changin length}}{\text{original length}}$

$$\varepsilon = \frac{\Delta L}{L}$$

Strain is thus, a measure of the deformation of the material and is a non dimensional Quantity i.e. it has no units. It is simply a ratio of two quantities with the same unit.

The engineering strain in compression is:

$$e = \frac{\Delta h}{h}$$

The true, or natural, strain in compression is given by

$$\varepsilon = \ln (e + 1)$$

When friction is present between the dies and the specimen, the metal adjacent to these regions undergoes little or no deformation.

Three dimensional state of strain: Consider an element subjected to three mutually perpendicular tensile stresses σ_x , σ_y and σ_z as shown in the figure below.

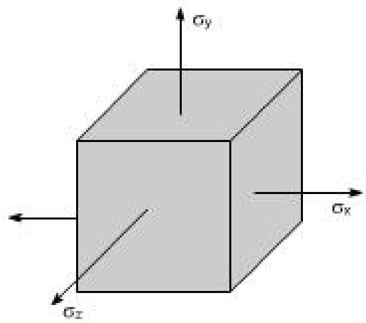

Figure 3.7 Three dimensional stress and strain applied

If σ_y and σ_z were not present the strain in the x direction from the basic definition of Young's modulus of Elasticity E would be equal to

$$\varepsilon_x = \sigma_x / E \text{ (Beer et al, 2013)}$$

The effects of σ_y and σ_z in x direction are given by the definition of Poisson's ratio 'v' to be equal as - $v\sigma_y$/ E and -$v\sigma_z$/ E

The negative sign indicating that if σ_y and σ_z are positive i.e. tensile, these they tend to reduce the strain in x direction thus the total linear strain is x direction is given by

$$\varepsilon_x = \frac{\sigma_x}{E} - \frac{\sigma_y}{E}v - \frac{\sigma_z}{E}v$$

$$\varepsilon_y = \frac{\sigma_y}{E} - \frac{\sigma_x}{E}v - \frac{\sigma_z}{E}v$$

$$\varepsilon_z = \frac{\sigma_z}{E} - \frac{\sigma_x}{E}v - \frac{\sigma_y}{E}v$$

In the compression test the sample was compressed towards the z direction and elongate the diameter. Due to these, it has the only two types of strains i.e. axial strain (ε_z) to wards z-axis and hoop strain (ε_θ) to changes the diameter.

$$\varepsilon_z = \frac{\Delta h}{h} \text{ (Beer et al, 2013)}$$

$$\varepsilon_\theta = \ln(\frac{D}{D_o})$$ (Beer et al, 2013)

Where h_f = final or after compassion of sample length, h_o = original or before compression of sample length, Δh = length of sample compressed, D_f = final sample diameter, D_o = original sample diameter and ΔD = diameter of sample elongated.

3.7 Numerical analysis and Simulation with DEFORM soft ware

In the given work the aim of finite element simulation was the identification of distribution of deformation characteristics within specimen volume. DEFORM is one of a Finite Element Method (FEM) based process simulation system designed to analyze various forming processes used by metal forming and related industries. In this work was to simulated compression test forming in the given dimension of specimen, and input constant value that is strength coefficient (K) and strain hardening exponent (n) for different percentage composition composite material to generated and process the compression running in the following steps. And determine strength coefficient (K) and strain hardening exponent (n) by using the following equations, n = $\Delta(\ln\sigma)/\Delta(\ln\varepsilon)$ and K = $\Delta\sigma/\Delta\varepsilon$.

Step 1. Define work piece geometry

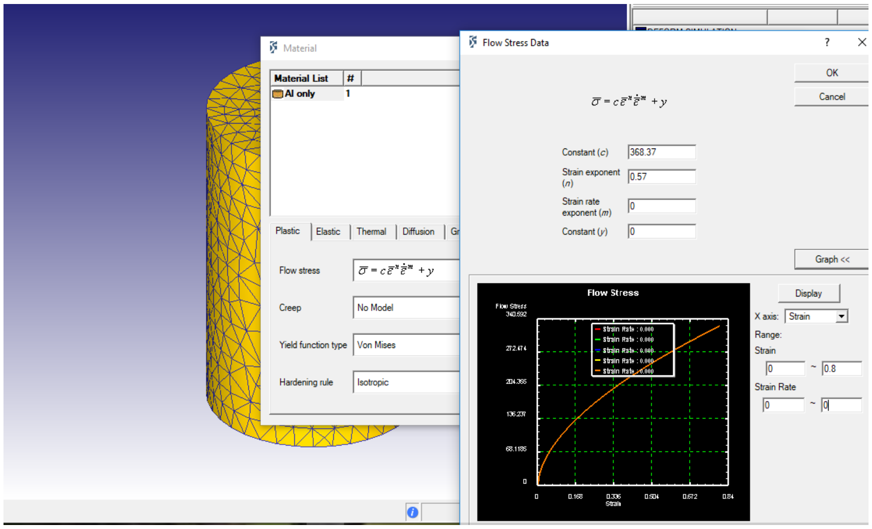

Figure 3.8 Numerical analysis for work piece geometry

Step 2 . Define top die geometry

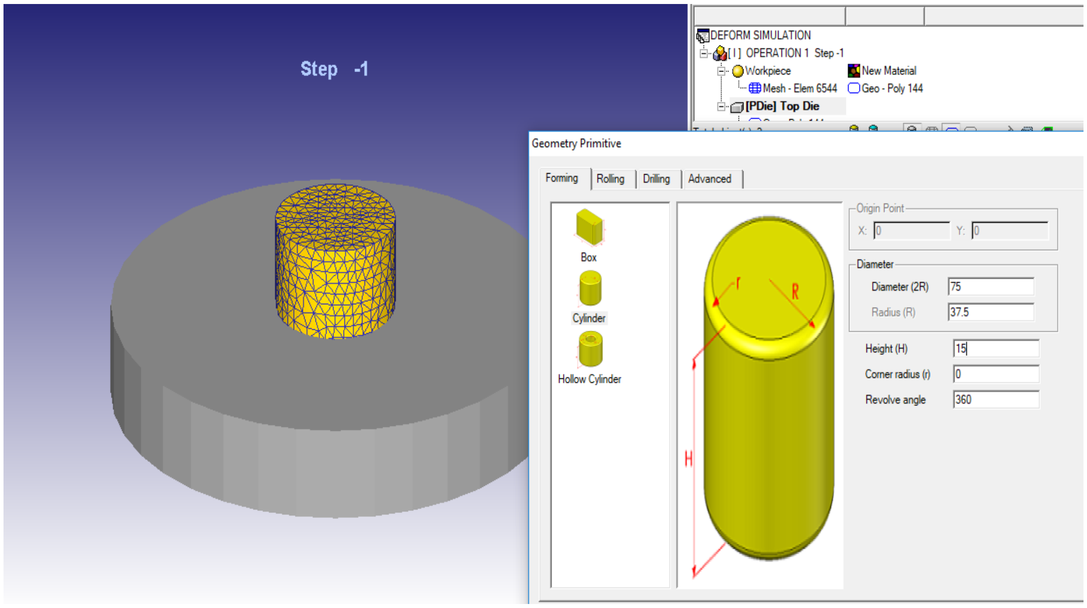

Figure 3.9 Numerical analysis for top die geometry

Step 3. Define bottom die geometry

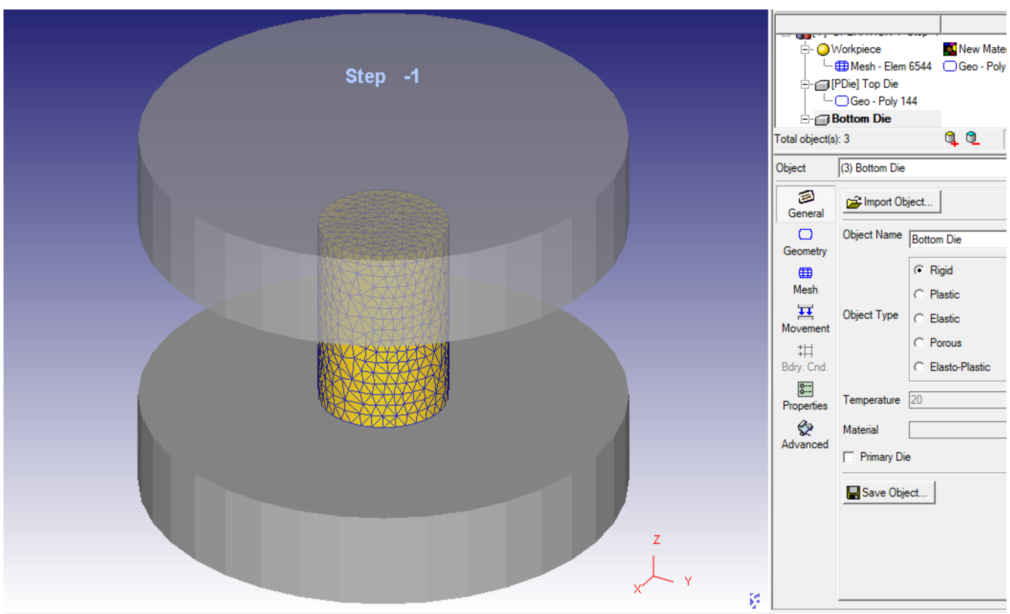

Figure 3. 10 Numerical analysis for bottom die geometry

Step 4. Run simulation

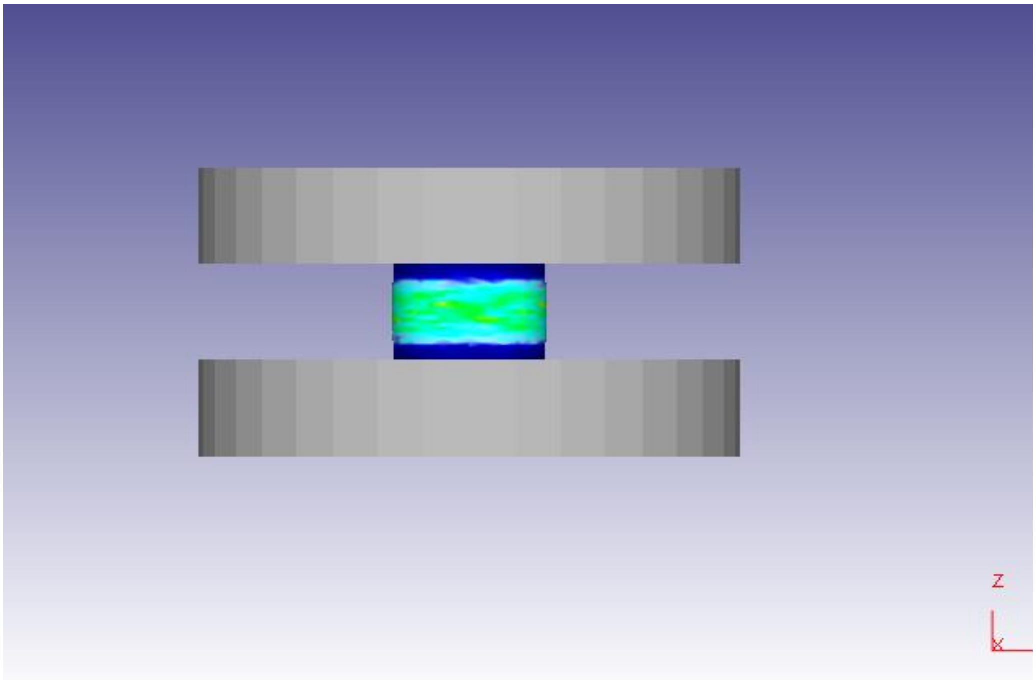

Figure 3.11 Numerical simulation for compression analysis

CHAPTER FORE

4. RESULT AND DESCATION

4.1 Introduction

Due to compression test the material tends to fracture where the load reached at the limited point. Actually the metal continues to strain harden all the way, so that the stress required to produce further deformation should also increase. If the true stress based on the actual cross-sectional area of the specimen is used, it is found that stress-strain curve increases continuously until plastic deformation occurs. If the strain measurement is also based on instantaneous measurement, the curve is called true stress-strain curve. It is also known as flow curve, since. It represents the basic plastics flow characteristics of the material. Many attempts have been made to fit mathematical equations to this curve. The plastic deformation is limited by plastic instability and fracture. In a certain point of the material, the effect of hardening is abrogated by the softening. The source of softening can be change of geometry, change of the strain rate and change of temperature. But in this work is cold working process, so the temperature is not affect to fracture the material only take change of geometry of specimen and change of the strain rate. The plastic deformation of stable if the force increases with increasing deformation. Therefore, due to the following compression test result and micro structure result as well as numerical simulation are generalized or conclude how to change from pure Aluminum to its composite material which are add to different percentage composition of Titanium diboride powder.

4.2 Compression test result

A compression test determines the characteristics of materials under pressing loads. The sample was compressed and deformation at various loads was noted. Compressive stress and strain was calculated and plotted as a stress-strain diagram which is used to determine fracture limit, proportional limit, yield strength and yield point. When a compressive load is applied on a specimen, the deformation may take place: for brittle materials it may be crushing or fracture and for ductile material it may be due to elastic or plastic. The following results, when the load applied the sample were deformed.

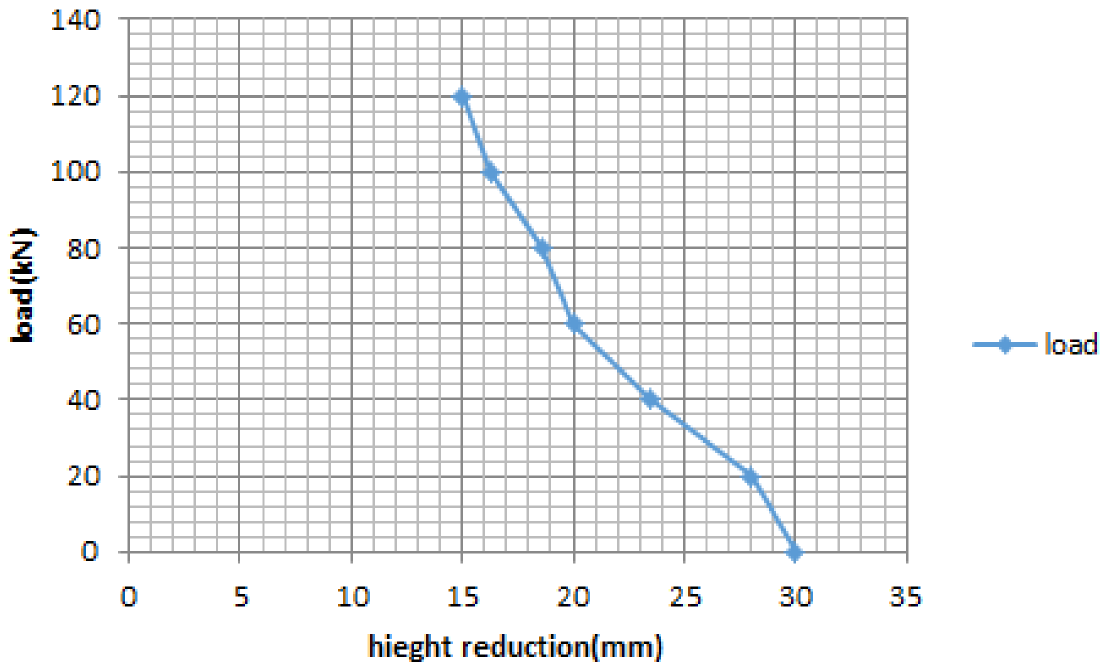

Figure 4. 1 Pure Aluminum Force with sample height graph in compression test

Table 4. 1 Pure Aluminum sample dimension and its strain value obtained by compression

Load (KN)	**D_o**	**D**	**h_o**	**h**	**Δh**	**ε_z**	**ε_θ**
0	20mm	20.00mm	30mm	30.00mm	0.00mm	0.000	0.000
20	20mm	20.85mm	30mm	28mm	2.00mm	0.067	0.042
40	20mm	21.05mm	30mm	23.5mm	6.50mm	0.220	0.051
60	20mm	21.84mm	30mm	20.04mm	9.96mm	0.331	0.088
80	20mm	22.00mm	30mm	18.6mm	11.4mm	0.380	0.095
100	20mm	25.23mm	30mm	16.3mm	13.7mm	0.460	0.232
120	20mm	28.36mm	30mm	15mm	15mm	0.750	0.349

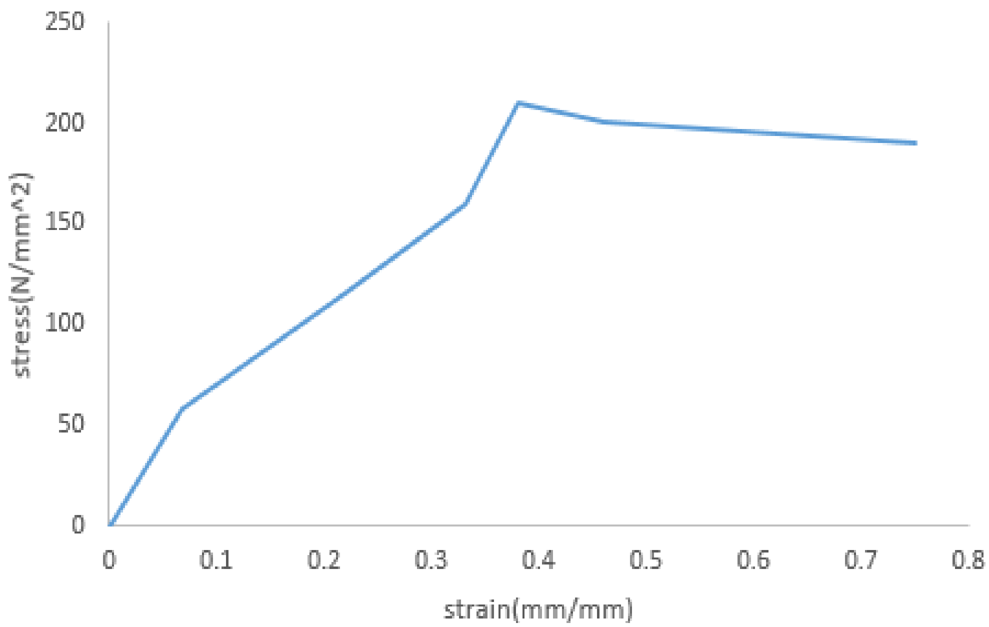

Figure 4. 2 Pure Aluminum stress -strain curve in compression test

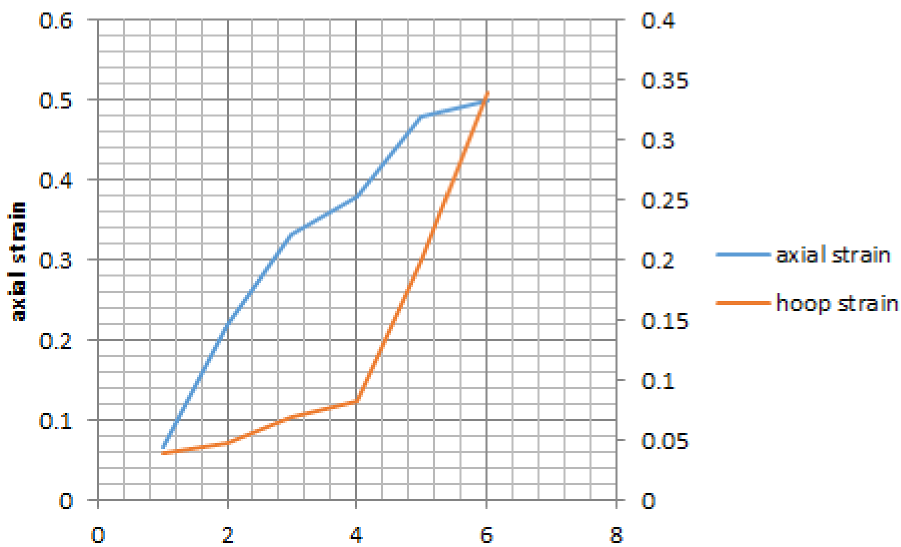

Figure 4. 3 pure aluminum axial and hoop strain discription

The height was decreased and the diameter was increased when the load was increased. Hence, the sample was fractured at the load 80kN, which give as the result maximum stress 210N/mm^2 and axial strain (**ε_z**) 0.38 as well as hoop strain (**ε_θ**) 0.095. As we have seen the graph the intersection of axial strain and hoop strain leads fracture point.

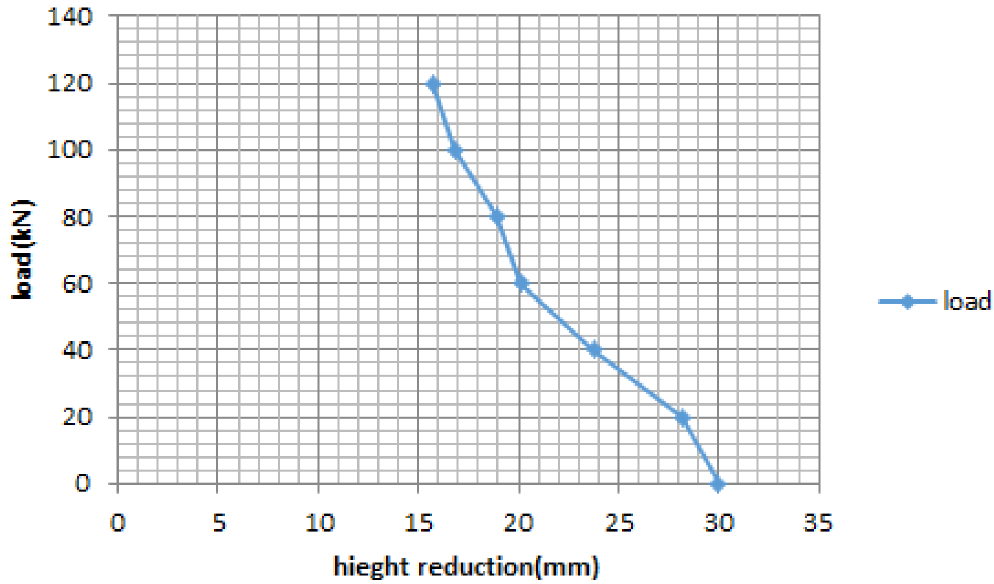

Figure 4. 4 Al-TiB_2 (4% TiB_2) Force with sample height graph in compression test

Table 4. 2 Al- 4%TiB_2 sample dimension and its strain value obtained by compression

Load (kN)	D_o	D	h_o	h	Δh	ε_z	ε_θ
0	20mm	20.00mm	30mm	30.00mm	0.00mm	0.00	0.00
20	20mm	20.65mm	30mm	28.20mm	1.80mm	0.06	0.032
40	20mm	20.97mm	30mm	23.8mm	6.20mm	0.21	0.047
60	20mm	21.42mm	30mm	20.12mm	9.88mm	0.33	0.069
80	20mm	21.70mm	30mm	18.93mm	11.07mm	0.37	0.082
100	20mm	24.4mm	30mm	16.81mm	13.79mm	0.46	0.199
120	20mm	27.35mm	30mm	15.70mm	14.30mm	0.48	0.313

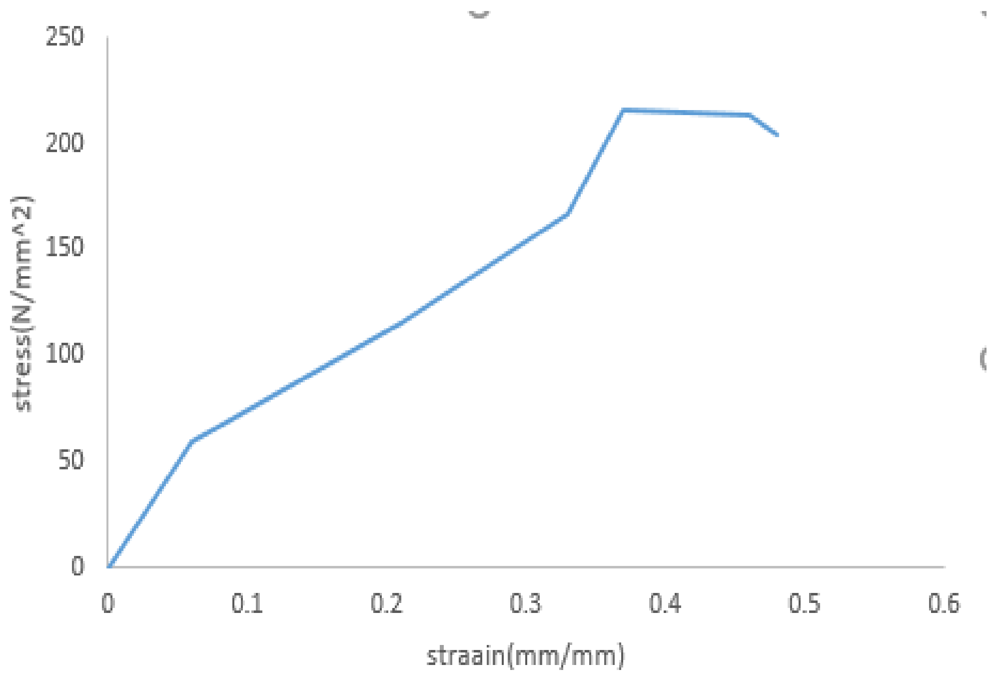

Figure 4. 5 Al-TiB_2 (4% TiB_2) stress - strain curve in compression test

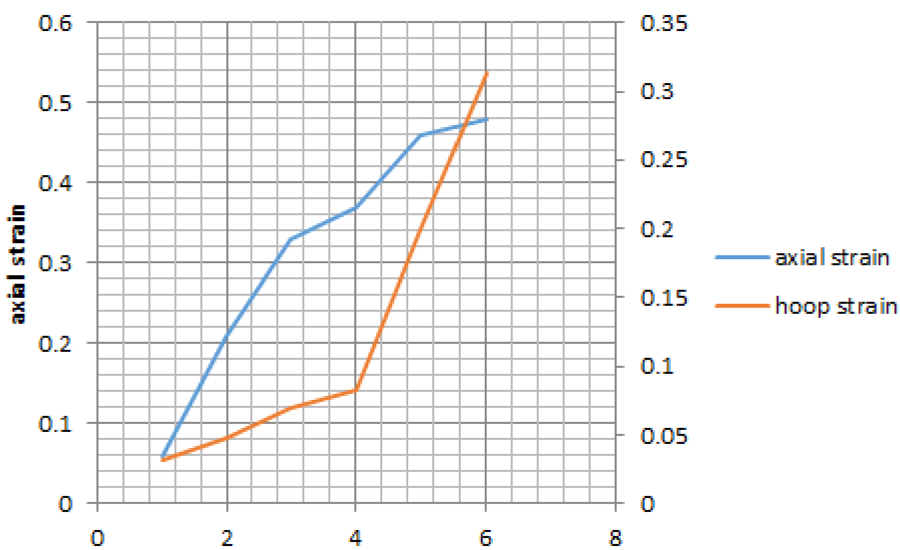

Figure 4.6 Al-TiB_2 (4% TiB_2) axial and hoop strain description

The height was decreased and the diameter was increased when the load was increased. Hence, the sample was fractured at the load 80kN, which give as the result maximum stress 216.31N/mm^2 and axial strain (**ε_z**) 0.37 as well as hoop strain (**ε_θ**) 0.082. As we have seen the graph the intersection of axial strain and hoop strain leads fracture point.

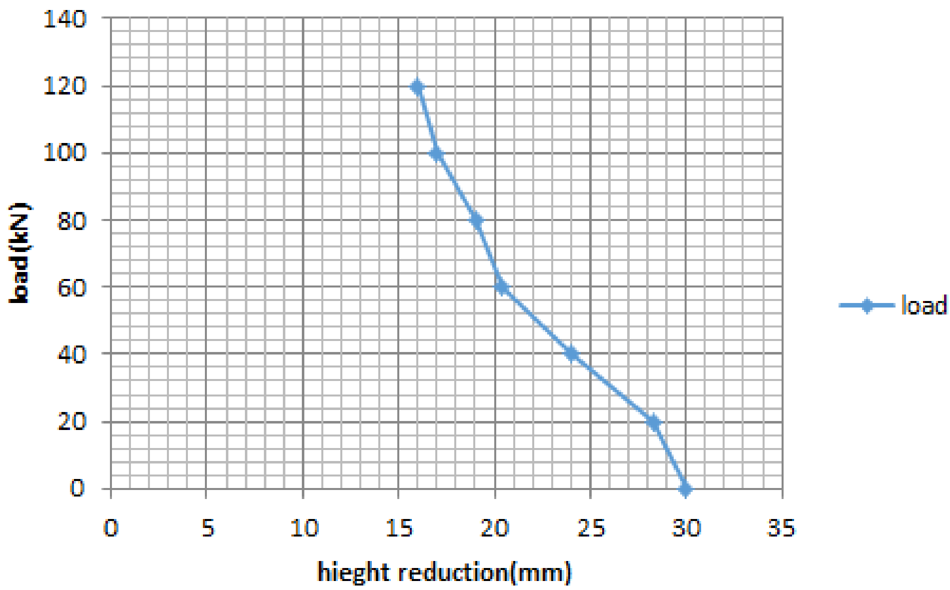

Figure 4.7 Al-TiB_2 (8% TiB_2) Force with sample height graph in compression test

Table 4. 3 Al- 8%TiB_2 sample dimension and its strain value obtained by compression

Load (KN)	**D_o**	**D**	**h_o**	**h**	**Δh**	**ε_z**	**ε_θ**
0	20mm	20.00mm	30mm	30.00mm	0.00mm	0.00	0.00
20	20mm	20.61mm	30mm	28.31mm	1.69mm	0.056	0.030
40	20mm	21.89mm	30mm	24.05mm	5.95mm	0.198	0.044
60	20mm	21.31mm	30mm	20.40mm	9.60mm	0.32	0.064
80	20mm	21.40mm	30mm	19.05mm	10.95mm	0.365	0.068
100	20mm	24.10mm	30mm	117.01mm	12.99mm	0.433	0.186
120	20mm	26.86mm	30mm	16.00mm	14.00mm	0.47	0.295

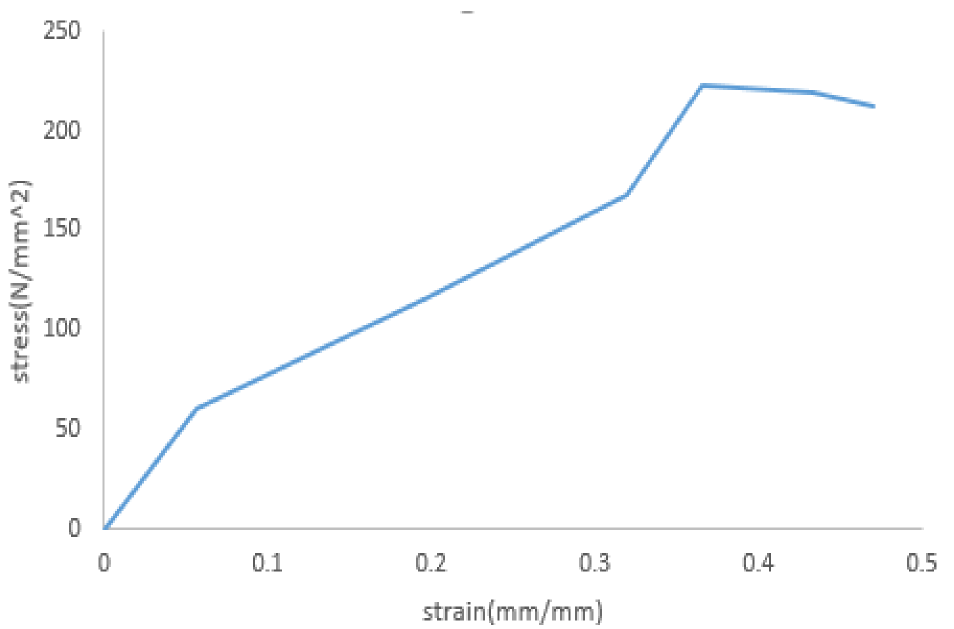

Figure 4.8 Al-TiB_2 (8% TiB_2) stress - strain curve in compression test

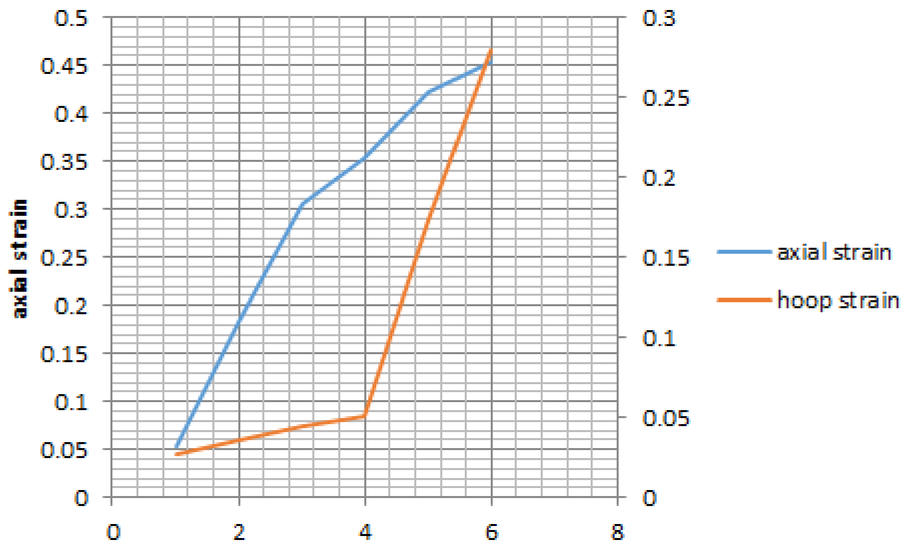

Figure 4.9 Al-TiB_2 (8% TiB_2) axial and hoop strain description

The height was decreased and the diameter was increased when the load was increased. Hence, the sample was fractured at the load 80kN, which give as the result maximum stress 222.42N/mm^2 and axial strain (**ε_z**) 0.365 as well as hoop strain (**ε_θ**) 0.068. As we have seen the graph the intersection of axial strain and hoop strain leads fracture point.

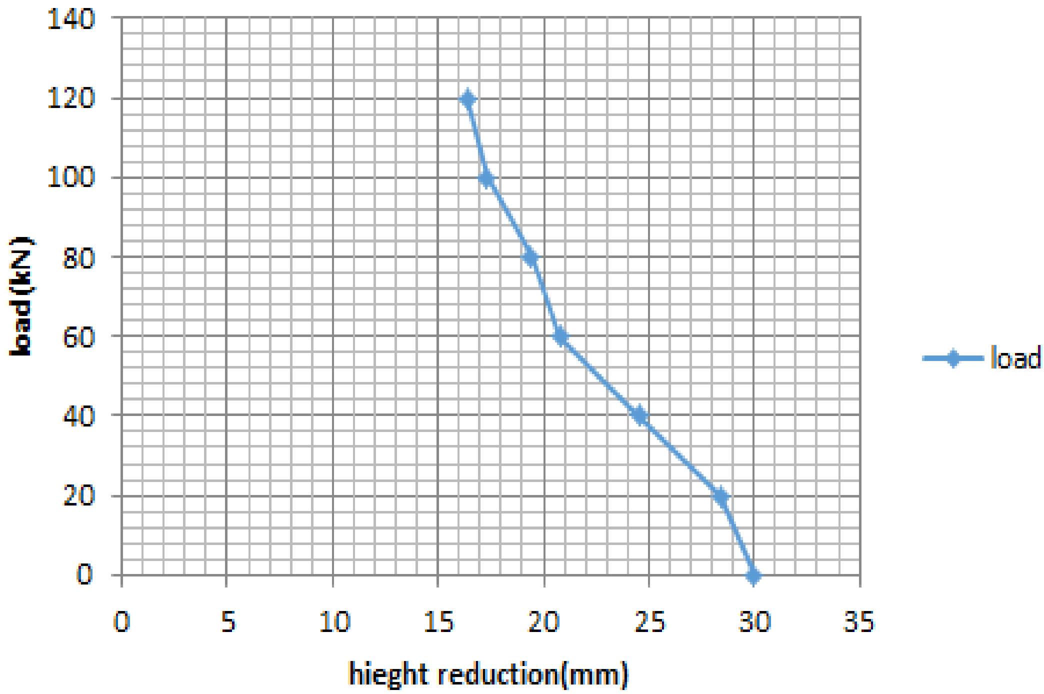

Figure 4.10 Al-TiB_2 (12% TiB_2) Force with sample height graph in compression test

Table 4. 4 Al- 12%TiB_2 sample dimension and its strain value obtained by compression

Load (KN)	D_o	D	h_o	h	Δh	ε_z	ε_θ
0	20mm	20.00mm	30mm	30.00mm	0.00mm	0.00	0.00
20	20mm	20.54mm	30mm	28.40mm	1.60mm	0.053	0.027
40	20mm	20.74mm	30mm	24.52mm	5.48mm	0.183	0.036
60	20mm	20.89mm	30mm	20.81mm	9.19mm	0.306	0.044
80	20mm	21.05mm	30mm	19.40mm	10.60mm	0.353	0.051
100	20mm	23.80mm	30mm	17.32mm	12.68mm	0.423	0.174
120	20mm	26.45mm	30mm	16.40mm	13.60mm	0.453	0.280

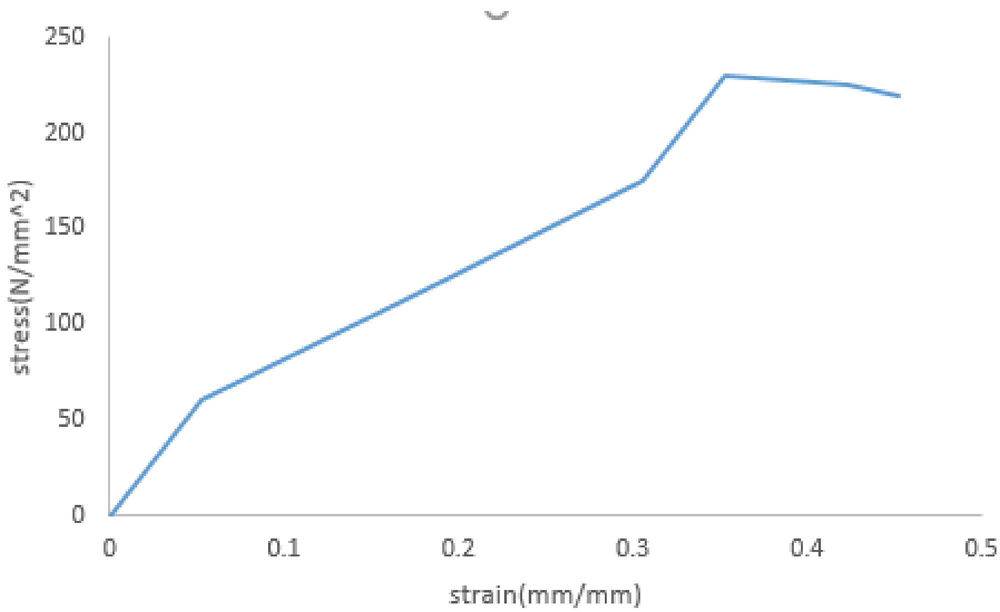

Figure 4.11 Al-TiB_2 (12% TiB_2) stress - strain curve in compression test

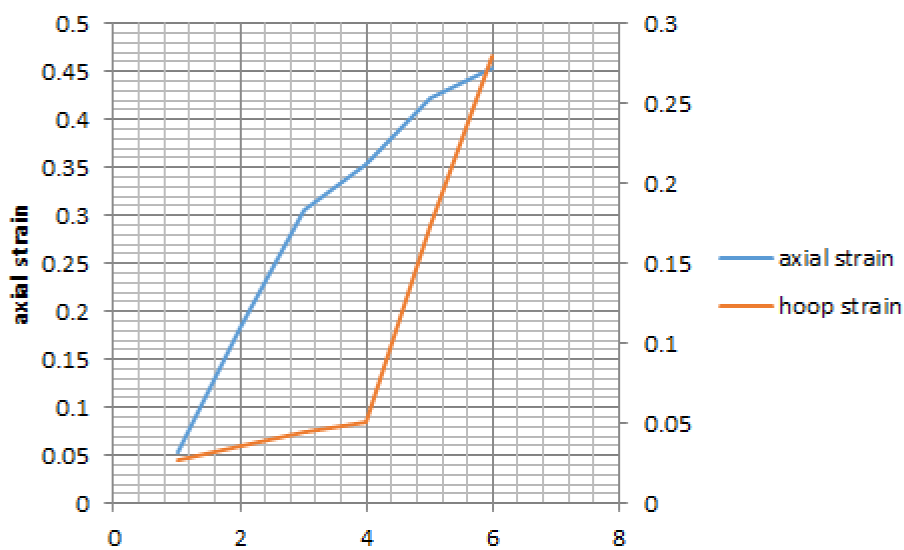

Figure 4.12 Al-TiB_2 (12% TiB_2) axial and hoop strain description

The height was decreased and the diameter was increased when the load was increased. Hence, the sample was fractured at the load 80kN, which give as the result maximum stress 229.88N/mm^2 and axial strain (ε_z) 0.353 as well as hoop strain (ε_θ) 0.051. As we have seen the graph the intersection of axial strain and hoop strain leads fracture point.

Generally, the stress was increased and both axial and hoop strain decreased when the percentage composition of Titanium diboride (TiB_2) was increased. Basically Al –TiB_2 (8% TiB_2) is best from other composition i.e. 0% TiB_2, 4% TiB_2, 12% TiB_2. Since, if the ceramic powder or the reinforcement was more, the property of the material would change from ductile in to brittle. So, as we have seen the result Al –TiB_2 (8% TiB_2) composite material is best to forming process.

4.3 Micro Structures and Micro hardness

1. Micro Structures

In Al 1350, the microstructure is composed of an aluminum matrix containing TiB_2 powder as reinforcement. In general the TiB_2 powder is not uniformly distributed, but tends to be connected at inter boundaries. By used Optical microscopy was created micro structure of the sample, it can be seen that the TiB_2 powder is not uniformly distributed, and most of TiB_2 accumulated at the grain boundaries is present in the form of particle. In the specimen produced by using a smaller size and prepared its process cutting the sample by with abrasive cutter machine, mounting to hold the sample by with polymer, grinding by with the different size glass paper, polishing, etching by with acidic chemical, and finally viewed the micro structure of the sample like the following image.

2. Micro hardness test

A micro hardness tester was used to measure the micro hardness of the specimens. This tester is capable of measuring two kinds of hardness, Vickers and Knoop. In this study, Vickers hardness was employed. According to the indentation diameter of the diamond indenture (pyramid shape) made on the surface of the samples, the value of micro-hardness can be read directly from a conversion tables provided by the manufacturer. For this micro-hardness measurement, the indentation load used was 5kg.f/mm^2 and 10kg.f/mm^2. The main objective was to study the effect of TiB_2 addition, and to measure the hardness of the matrix. In forming materials the hardness HV values don't exceed 130 and 260 for the indentation load 5kg.f/mm^2 and 10kg.f/mm^2 respectively. Therefore, *Al –TiB_2 (8% TiB_2) composite material is best formability*, as we have seen appendix C.

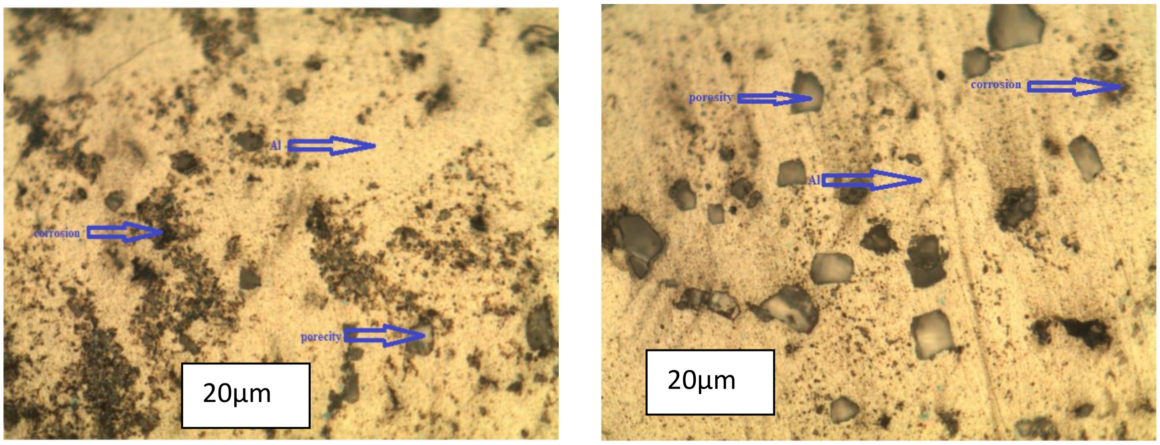

Figure 4.13 Pure Aluminum micro structure

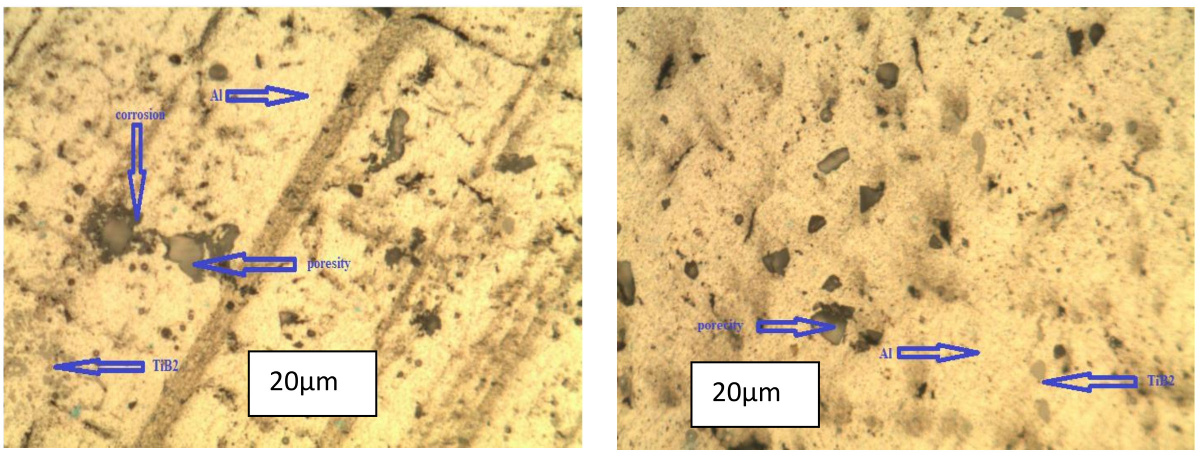

Figure 4.14 Al –TiB_2 (4% TiB_2) micro structure

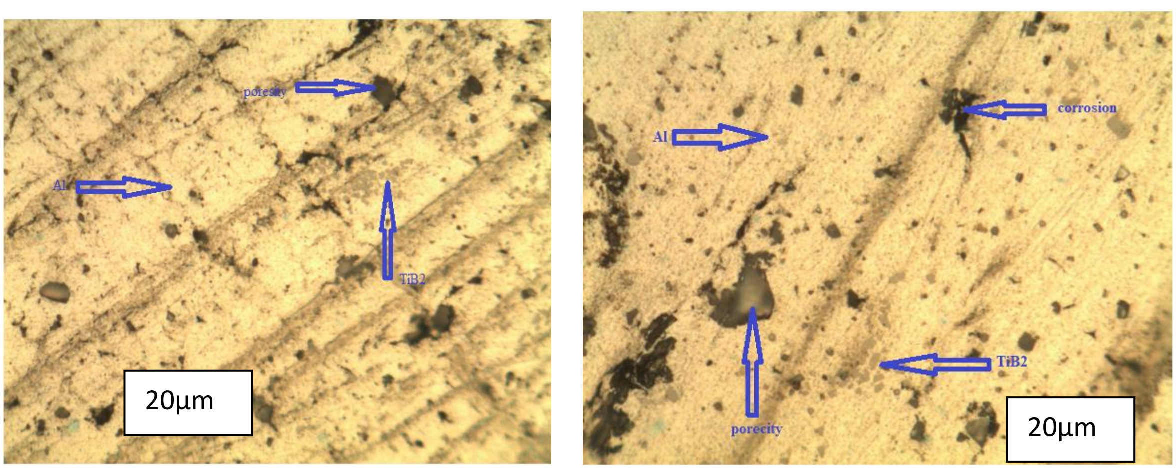

Figure 4.15 Al –TiB_2 (8% TiB_2) micro structure

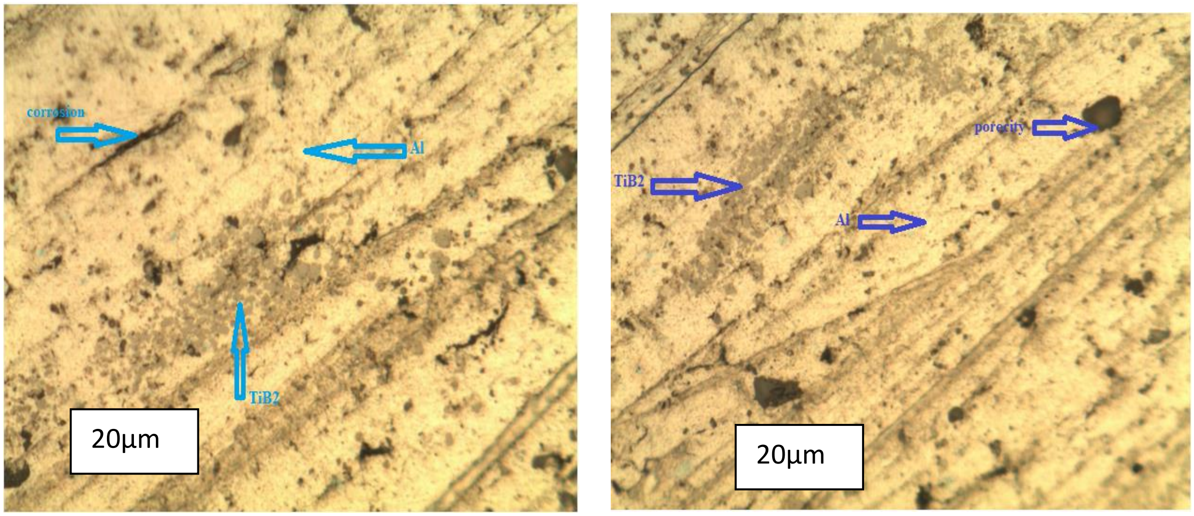

Figure 4.16 Al –TiB_2 (12% TiB_2) micro structure

4.4 Numerical simulation

Table 4. 5 values of strength coefficient and strain hardening exponent

Sample	Value of K (N/mm^2)	Value of n
Al- TiB_2 (0% TiB_2)	368.37	0.57
Al- TiB_2 (4% TiB_2)	394	0.53
Al- TiB_2 (8% TiB_2)	417.35	0.53
Al- TiB_2 (12% TiB_2)	446.46	0.54

Pure Aluminum

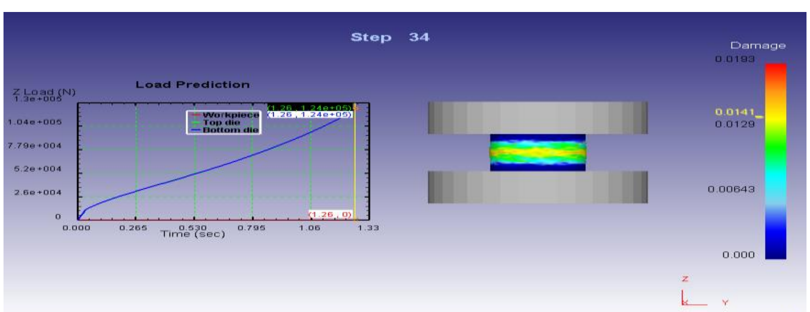

Figure 4.17 Showing damage condition and load with time graph for pure aluminum

Due to compression when the load increases the sample going to damage or fracture at the middle (yellow) part of the sample as we shown the above figure 4. 17.

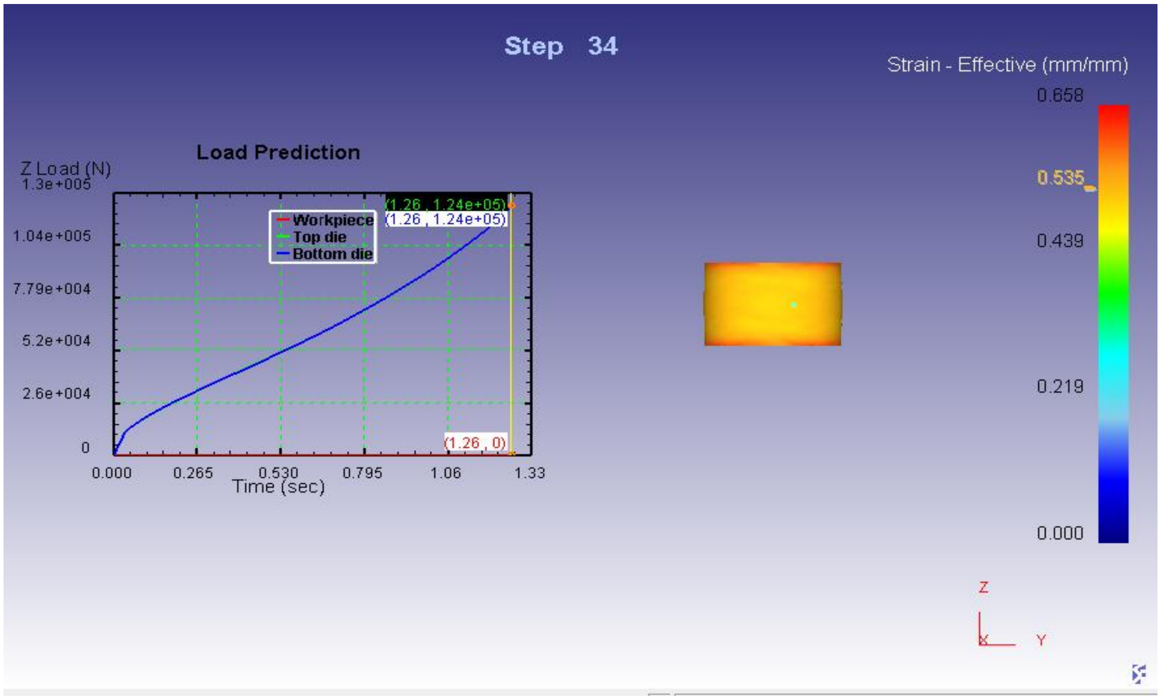

Figure 4.18 Strain effective for pure aluminum

Due to compression when the load increases the sample going to damage or fracture and the strain value is increase i.e. at 80KN load the strain value is maximum which is 0.410 as shown the above figure 4. 18.

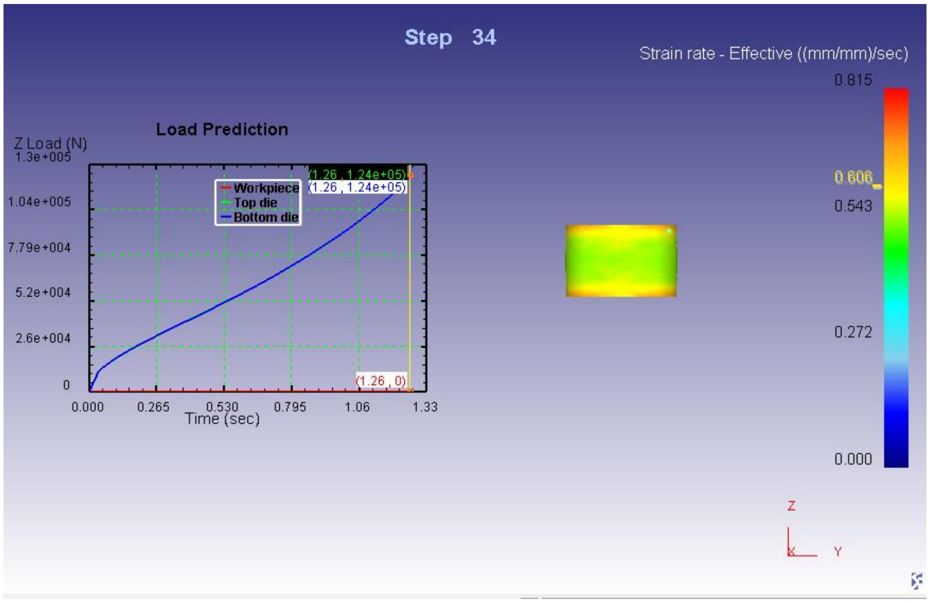

Figure 4.19 Strain rate effective for pure aluminum

Due to compression when the load increases the sample going to damage or fracture and the strain rate value is increase i.e. at 80KN load the strain rate value is maximum which is 0.606 as shown the above figure 4. 19.

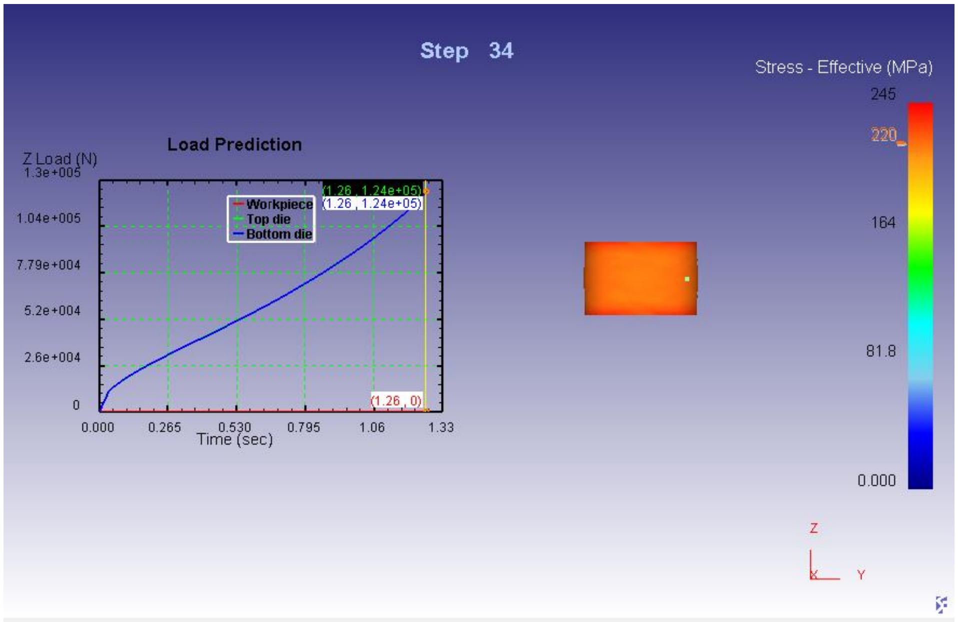

Figure 4.20 Stress effective pure aluminum

Due to compression when the load increases the sample going to damage or fracture and the stress value is increase i.e at 80KN load the strain rate value is maximum which is 220MPa as shown the above figure 4. 20.

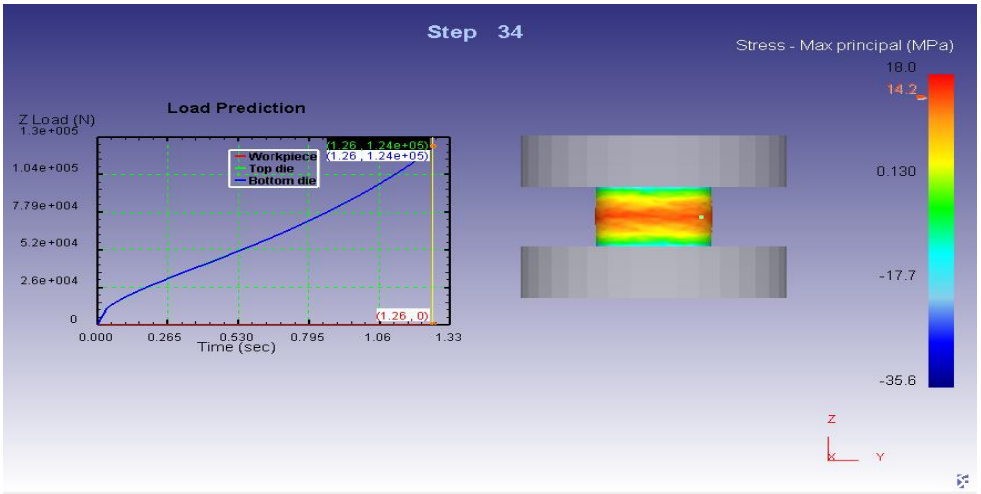

Figure 4.21 Stress max principal for pure aluminum

Due to compression when the load increases the sample going to damage or fracture and the stress maximum principal value is increase i.e. at 80KN load the strain rate value is maximum which is 14.2MPa as shown the above figure 4. 21.

Generally, the sample height decreased and diameter increased when the load was increased. Hence, the sample was fractured at the load 80kN applied which give as the result maximum stress 220N/mm^2 and strain 0.410.

4% Titanium diboride

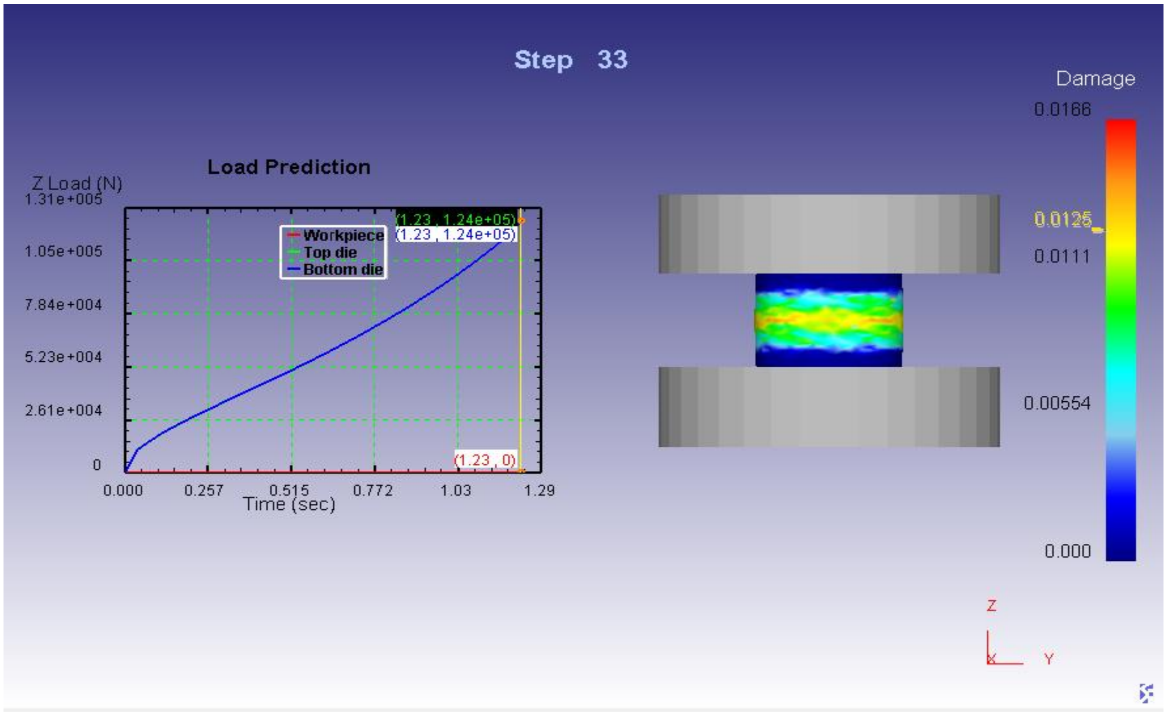

Figure 4.22 Showing damage condition and load with time graph for Al- TiB_2 (4% TiB_2)

Due to compression when the load increases the sample going to damage or fracture at the middle (yellow) part of the sample as we shown the above figure 4. 22.

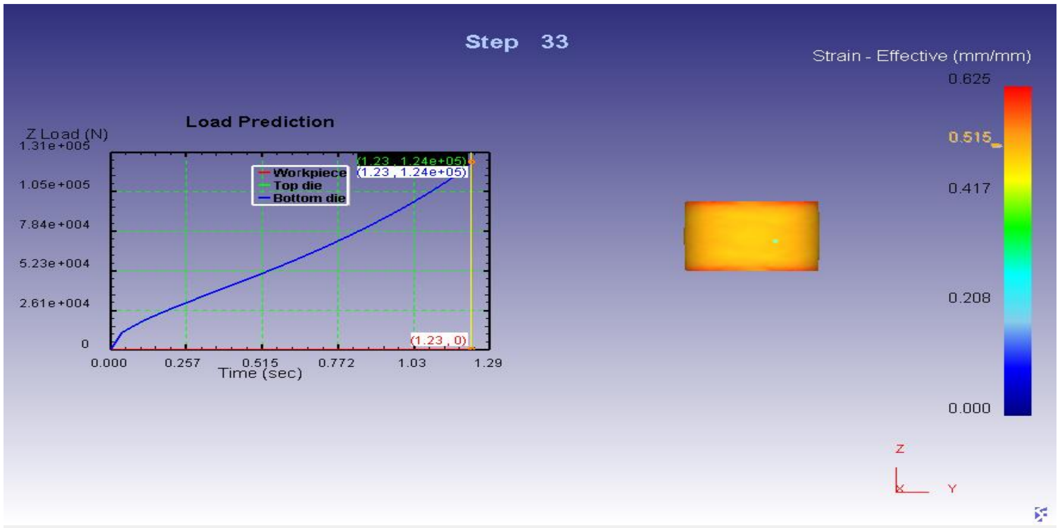

Figure 4.23 Strain effective for Al- TiB_2 (4% TiB_2)

Due to compression when the load increases the sample going to damage or fracture and the strain value is increase i.e. at 80KN load the strain value is maximum which is 0.400 as shown the above figure 4. 23.

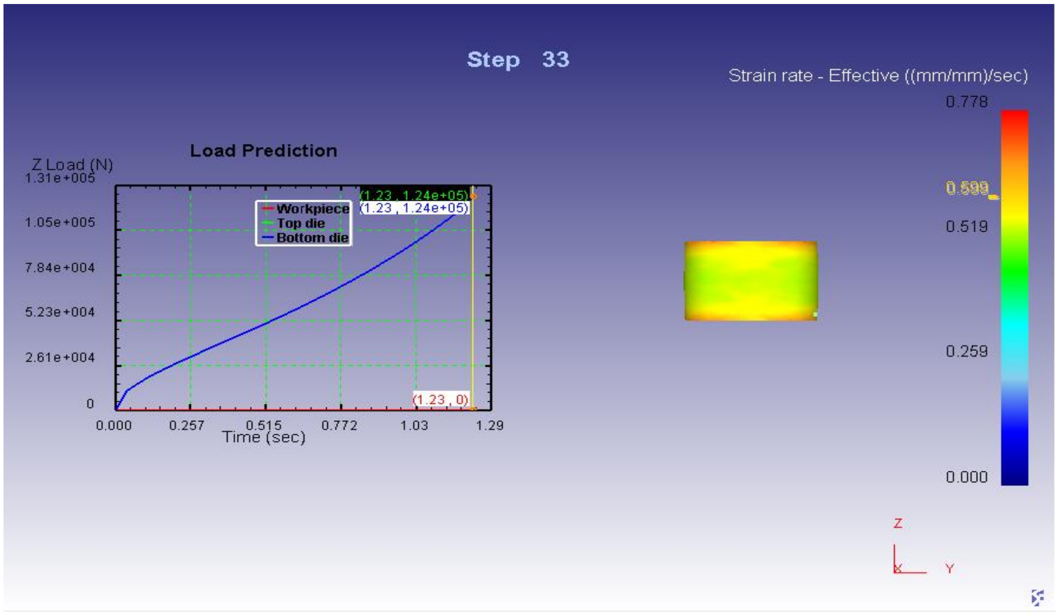

Figure 4.24 Strain rate effective for Al- TiB_2 (4% TiB_2)

Due to compression when the load increases the sample going to damage or fracture and the strain rate value is increase i.e. at 80KN load the strain rate value is maximum which is 0.599 as shown the above figure 4. 24

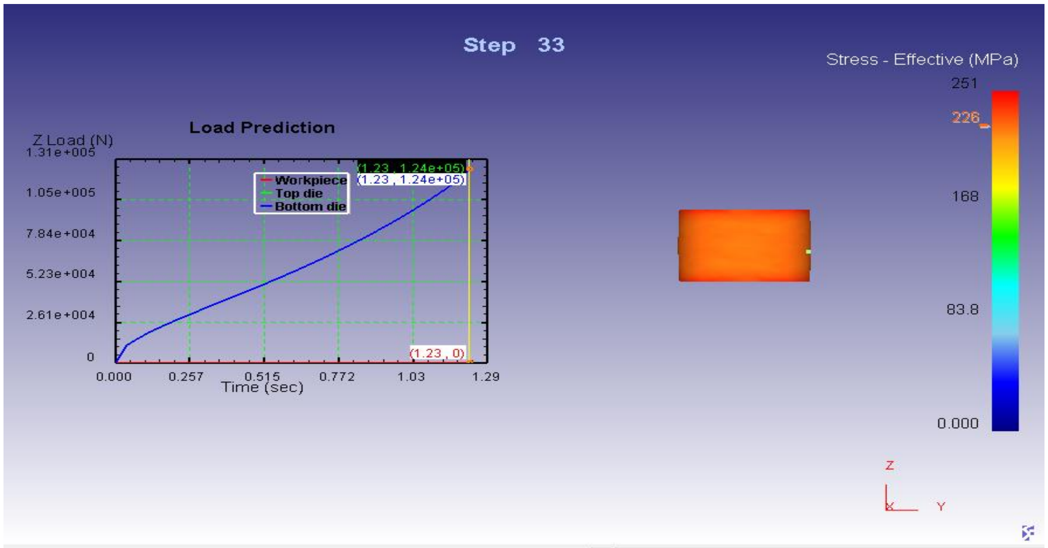

Figure 4.25 Stress effective for Al- TiB_2 (4% TiB_2)

Due to compression when the load increases the sample going to damage or fracture and the stress value is increase i.e. at 80KN load the strain rate value is maximum which is 226MPa as shown the above figure 4. 25.

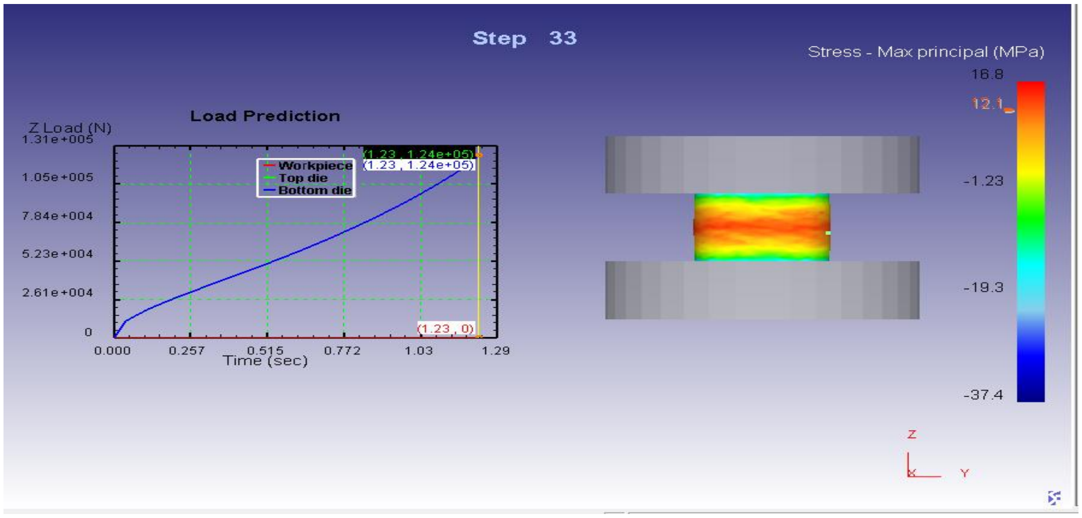

Figure 4.26 Stress max principal for Al- TiB_2 (4% TiB_2)

Due to compression when the load increases the sample going to damage or fracture and the stress maximum principal value is increase i.e. at 80KN load the strain rate value is maximum which is 12.1MPa as shown the above figure 4. 26.

Generally, the sample height decreased and diameter increased when the load was increased. Hence, the sample was fractured at the load 80kN applied which give as the result maximum stress 226N/mm^2 and strain 0.400.

8% Titanium diboride

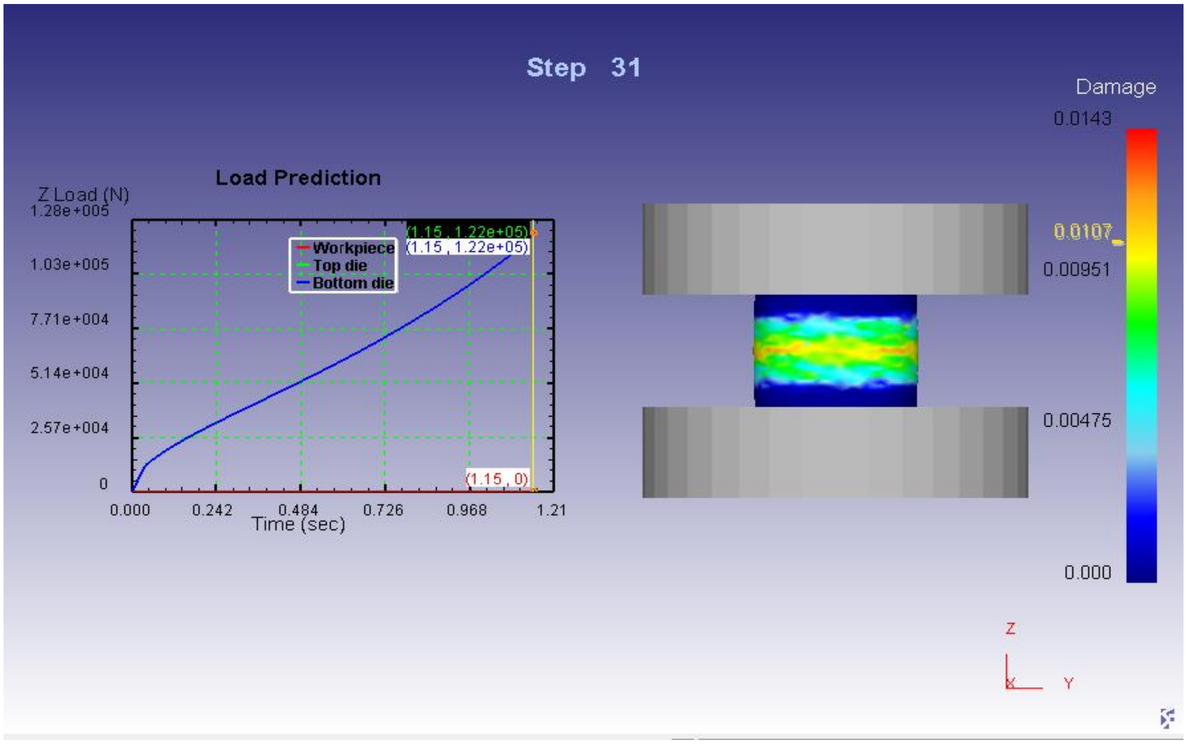

Figure 4.27 Showing damage condition and load with time graph for Al- TiB_2 (8% TiB_2)

Due to compression when the load increases the sample going to damage or fracture at the middle (yellow) part of the sample as we shown the above figure 4. 27.

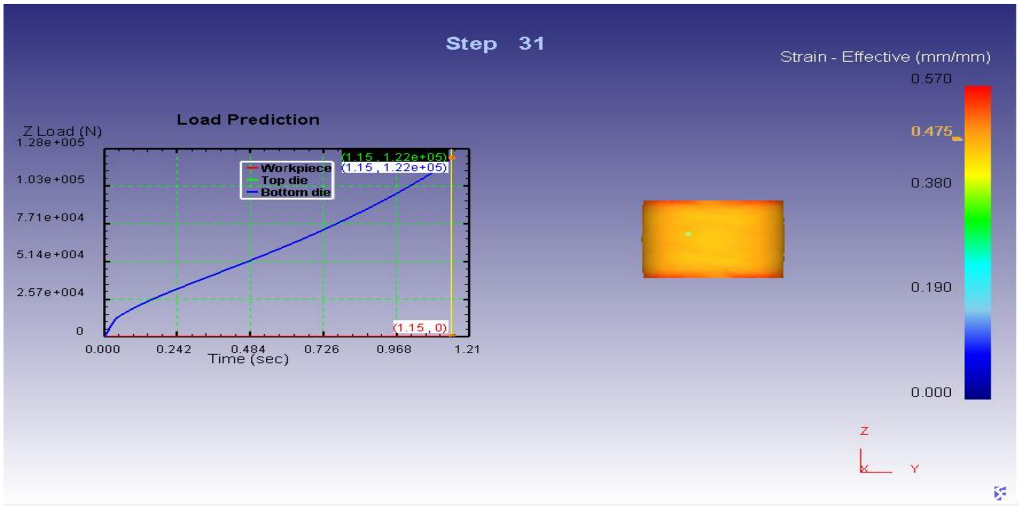

Figure 4.28 Strain effective for Al- TiB_2 (8% TiB_2)

Due to compression when the load increases the sample going to damage or fracture and the strain value is increase i.e. at 80KN load the strain value is maximum which is 0.380 as shown the above figure 4. 28.

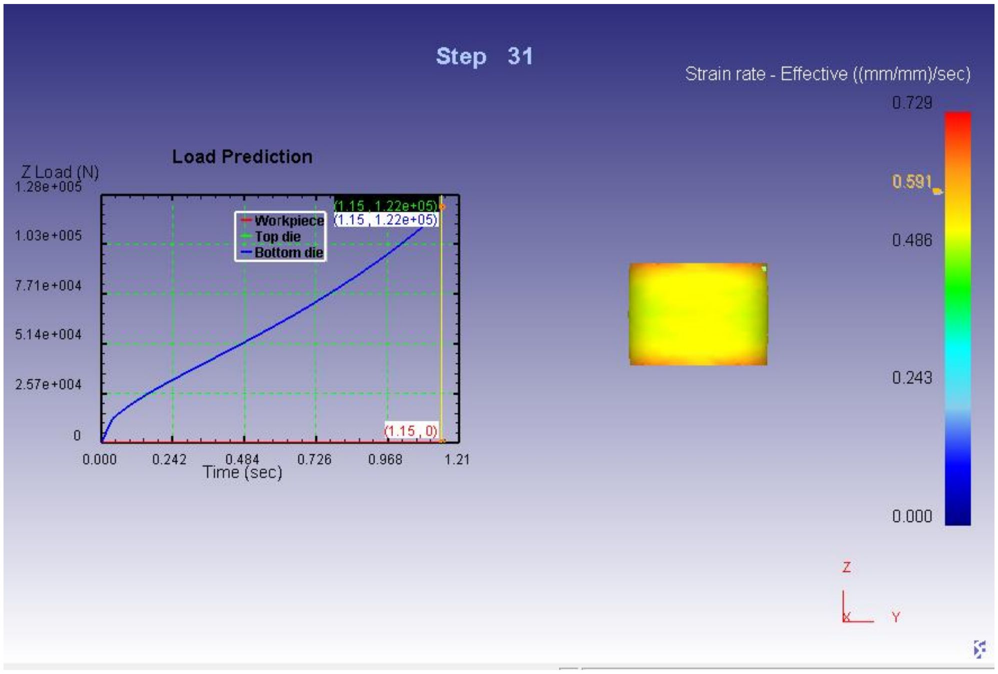

Figure 4.29 Strain rate effective for Al- TiB_2 (8% TiB_2)

Due to compression when the load increases the sample going to damage or fracture and the strain rate value is increase i.e. at 80KN load the strain rate value is maximum which is 0.591 as shown the above figure 4. 29.

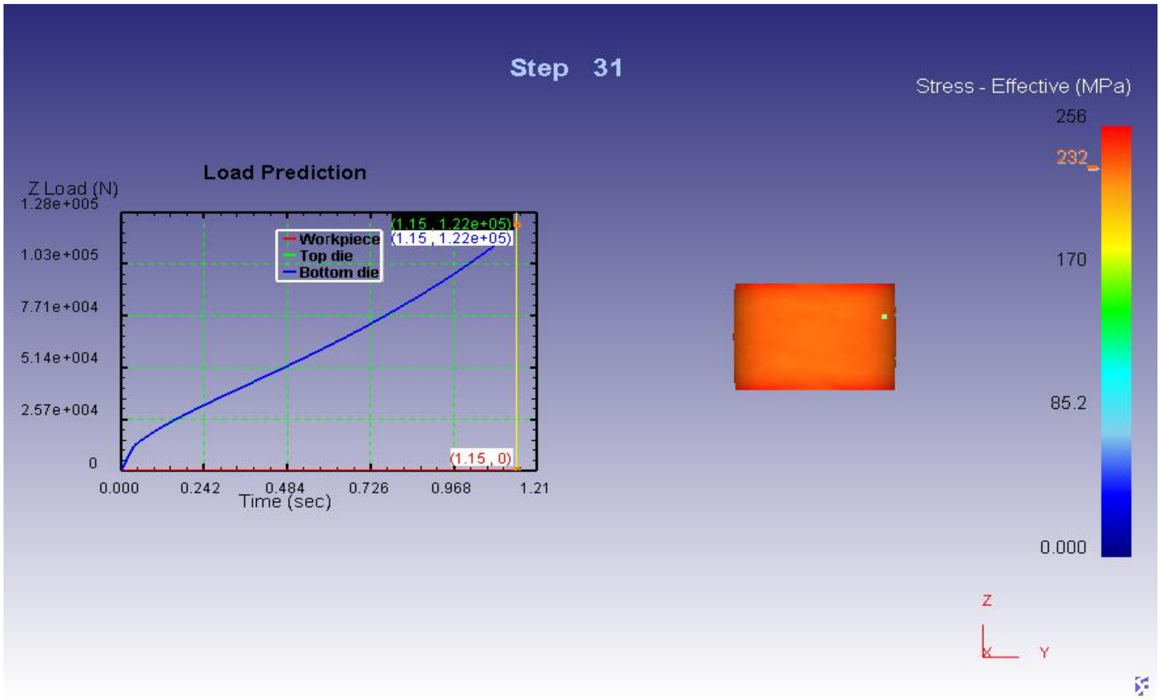

Figure 4.30 Stress effective Al- TiB_2 (8% TiB_2)

Due to compression when the load increases the sample going to damage or fracture and the stress value is increase i.e. at 80KN load the strain rate value is maximum which is 232MPa as shown the above figure 4. 30.

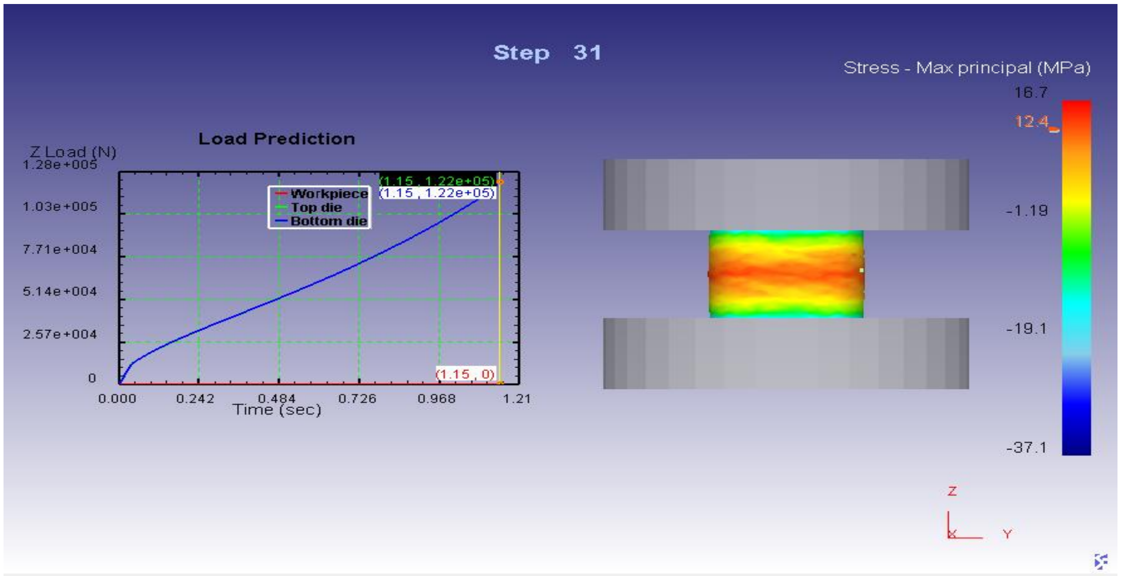

Figure 4.31 Stress max principal for Al- TiB_2 (8% TiB_2)

Due to compression when the load increases the sample going to damage or fracture and the stress maximum principal value is increase i.e. at 80KN load the strain rate value is maximum which is 12.4MPa as shown the above figure 4. 31.

Generally, the sample height decreased and diameter increased when the load was increased. Hence, the sample was fractured at the load 80kN applied which give as the result maximum stress 232N/mm^2 and strain 0.380.

12% Titanium diboride

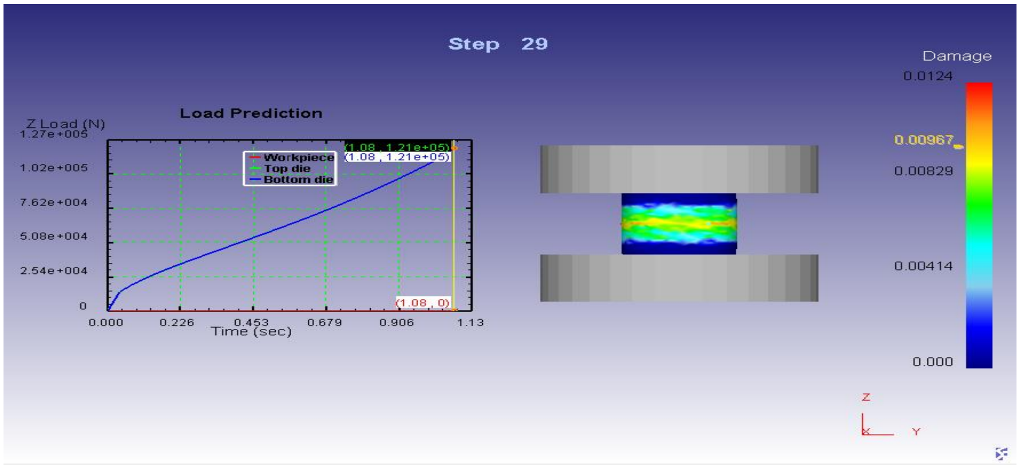

Figure 4.32 Showing damage condition and load with time graph for Al- TiB_2 (12% TiB_2)

Due to compression when the load increases the sample going to damage or fracture at the middle (yellow) part of the sample as we shown the above figure 4. 32.

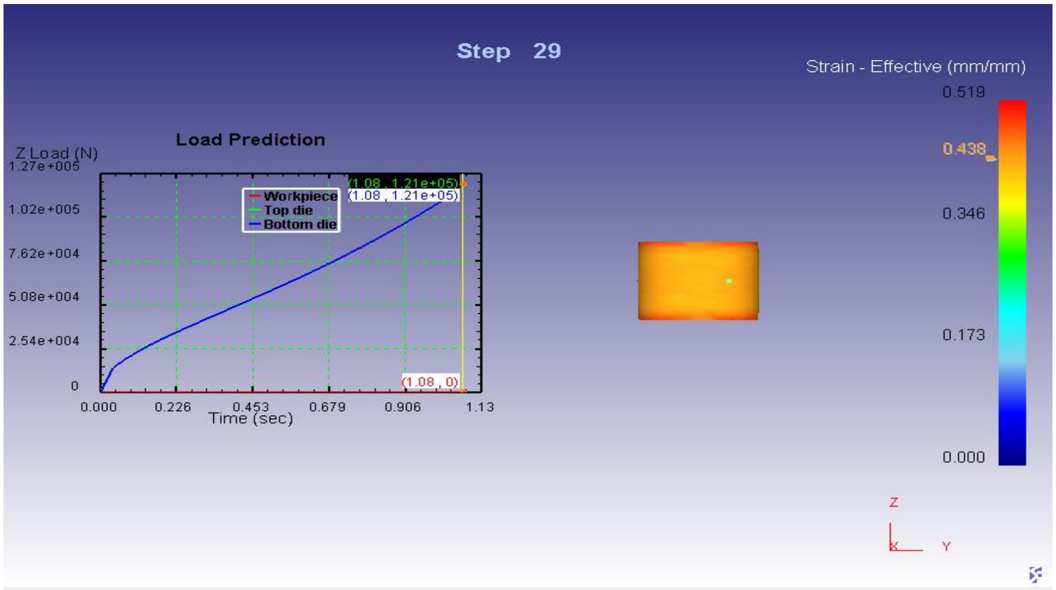

Figure 4.33 Strain effective for Al- TiB_2 (12% TiB_2)

Due to compression when the load increases the sample going to damage or fracture and the strain value is increase i.e. at 80KN load the strain value is maximum which is 0.360 as shown the above figure 4. 33.

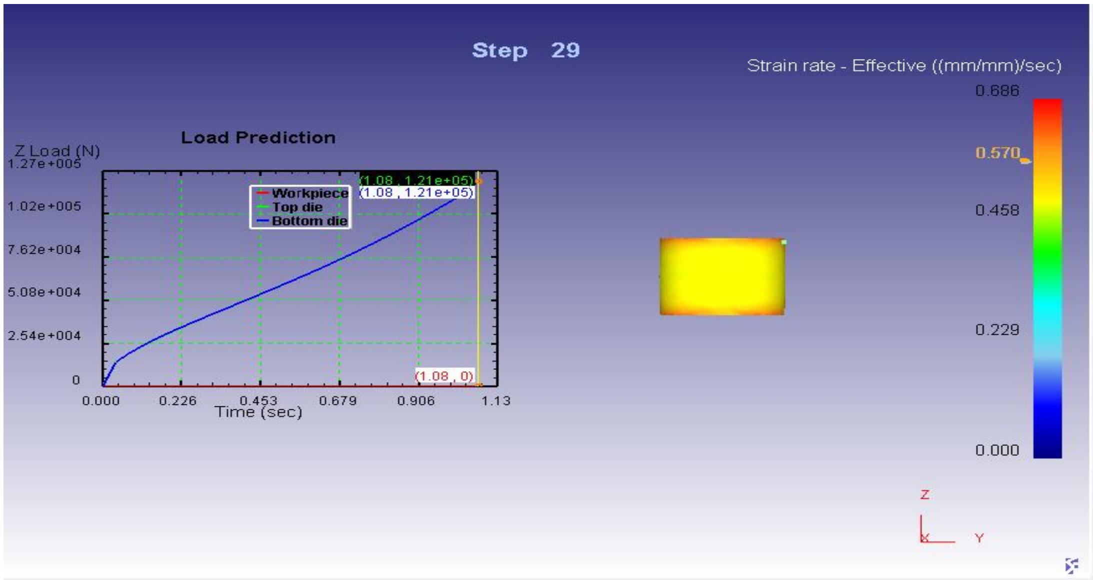

Figure 4.34 Strain rate effective for Al- TiB_2 (12% TiB_2)

Due to compression when the load increases the sample going to damage or fracture and the strain rate value is increase i.e. at 80KN load the strain rate value is maximum which is 0.570 as shown the above figure 4. 34.

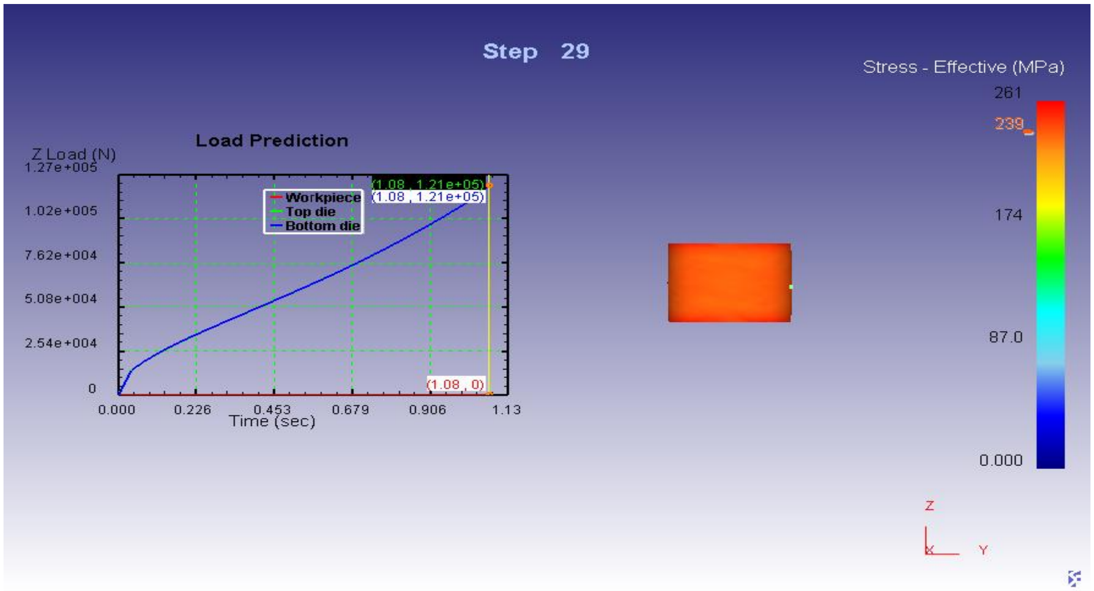

Figure 4.35 Stress effective Al- TiB_2 (12% TiB_2)

Due to compression when the load increases the sample going to damage or fracture and the stress value is increase i.e. at 80KN load the strain rate value is maximum which is 239MPa as shown the above figure 4. 35.

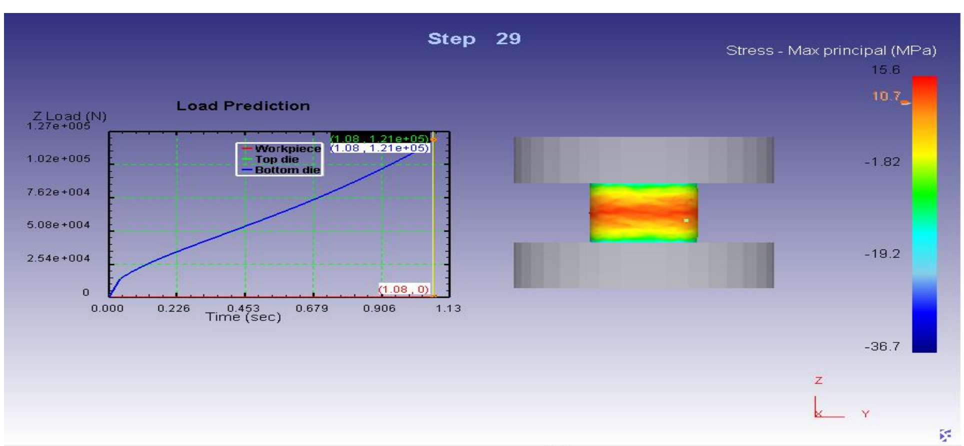

Figure 4.36 Stress max principal for Al- TiB_2 (12% TiB_2)

Due to compression when the load increases the sample going to damage or fracture and the stress maximum principal value is increase i.e. at 80KN load the strain rate value is maximum which is 10.7MPa as shown the above figure 4. 36.

Generally, the sample height decreased and diameter increased when the load was increased. Hence, the sample was fractured at the load 80kN applied which give as the result maximum stress 239N/mm^2 and strain 0.360.

The verification stress was increased and both axial and hoop strain decreased when the percentage composition of Titanium diboride (TiB_2) was increased. The experiment of this work is valid or correct because, when compere to the numerical simulation analysis the error was less than 10% between them. The following table is the comparison for experimental work and numerical simulation analysis at the maximum load 80KN.

Table 4. 6 the comparison between experimental work and numerical simulation analysies

composition	Experimental work		Numerical simulation		Error in %	
	stress(Mpa)	strain	Stress(Mpa)	strain	stress	strain
Al- TiB_2(0%TiB_2)	210.45	0.380	220	0.410	4.34	7.32
Al- TiB_2(4%TiB_2)	216.31	0.370	226	0.400	4.29	7.5
Al- TiB_2(8%TiB_2)	222.42	0.365	232	0.380	4.13	3.9
Al- TiB_2(12%TiB_2)	229.88	0.353	239	0.360	3.82	1.94

5. CONCLUSION, RECOMMENDATIONS AND FUTURE WORK

5.1 Conclusion

The following conclusions can be formulated based on the conducted investigations:

1. Fabricating cast Aluminum Matrix Composites by using the stir casting method has proved to be successful placing all substances together for melting is experimentally a very suitable process. During the initial stage of heating to about 660°C any moisture in the Titanium diboride powder and the pure Aluminum is burnt off and thus reduce the level of porosity. This advantage cannot be achieved by other methods in which the ceramic particles are introduced in the molten matrix materials from the top.

2. The addition of Titanium diaboride powder (TiB_2) to pure aluminum considerably increases formability of the composite, especially the yield point and fracture point.

3. Since, if the ceramic powder or the reinforcement was more, the property of the material would change from ductile in to brittle. So, as we have seen the result Al –TiB_2 (8% TiB_2) composite material is best to forming process.

4. Microstructural observation suggests that the stirring action of produces cast Al –TiB_2 with smaller grain size compared to an unstirred one Stirring breaks the dendrite structures into a small equaixed or chilled-type structure. The addition of ceramic particles, was coupled with the smaller grain size are factors that strengthen the matrix.

5.2 Recommendation

Research areas in cast MMC are broad several areas regarding the proposed fabrication method which excellence study, or development in more detail, include

1. The effect of stirrer and stirring speeds, it may be feasible to reduce particle fracture, further improve wetting, and minimize porosity through improved understanding of the process of mechanical stirring.

2. During casting the melting temperature was not notable because of lake of electrical furnace.

3. The microstructure and phase composition of the composite produced Variations in stirring and casting temperature can influence chemical reactions, and micro structure was not visible for with optical microscope used magnified to 20 micro meter.

5.3 Future work

The present study can be as one of the fundamental researches for formability behavior of MMC. Therefore, improving and following this study can be considered in future works. Directions of the future research are to investigate the formability behavior of Aluminum-Titanium diboride composite material because this material has high forming behavior, high strength and high corrosion resistance material. Therefore, customers need for this material for the future as the direction of the research. The work could be done by considering stirrer speed, melting temperature composition rate in fabrication time and fracture strain, stress and fracture point developed between them.

6. REFERENCES

Atturan, U. A., Nandam, S. H., Murty, B. S., & Sankaran, S. (2017). Deformation behavior of in-situ TiB_2 reinforced A357 aluminum alloy composite foams under compressive and impact loading. Materials Science and Engineering: A, 684, 178-185.

Balachandar, R., Balasundaram, R., & Rajkumar, G. (2018, February). Dry Sliding Wear Characteristics of Aluminum 6061-T6, Magnesium AZ31 and Rock Dust Composite. In IOP Conference Series: Materials Science and Engineering (Vol. 314, No. 1, p. 012013).

Beer, F. P., DeWolf, J. T., & Johnston Jr, E. R. (2013). Estática e mechanical dos materials. AMGH Editora.

Cobden, R., & Banbury, A. (1994). Aluminum: physical properties, characteristics and alloys. Talat lecture, 1501(11), 144-155.

Darabi, R., Azodi, H. D., & Bagherzadeh, S. (2017). Investigation into the effect of material properties and arrangement of each layer on the formability of bimetallic sheets. Journal of Manufacturing Processes: 29, 133-148.

Davey, S., Cantwell, W., Das, R., & Kalyanasundaram, S. (2012). Investigation into the formability of carbon fiber/polyether ether ketone composite sheets in stamp forming processes.

Emamy, M., Mahta, M., & Rasizadeh, J. (2006). Formation of TiB_2 particles during dissolution of TiAl3 in Al–TiB2 metal matrix composite using an in situ technique. Composites science and Technology: 66(7-8), 1063-1066.

Himanshu Kala, K.K.S Mer, Sandeep Kumar (2014). A Review on Mechanical and Tribological Behaviors of Stir Cast Aluminum Matrix Composites. Procedia Materials Science 6, 1951 – 1960

Hollomon R., Munro, R. G., Lee, D. N. (2008). metal forming technology. Fundamentals of Metalworking 16(2), 440-450.

Hosamani, G.G., Vishal B. manoji, Vishwanath R. Biradar, Venkatesh N. Kallappagol, Laxmi I. Haragapure, Characterization of silicon carbide reinforced aluminum matrix composites by using stir casting method. International Journal of Mechanical and Production Engineering, (2016) 2320-2092

Hu, H.E., Xin-yunWang, Lei Deng, High temperature deformation behavior and optimal hot processing parameters of Al–Si eutectic alloy. Materials Science & Engineering A576 (2013)45-51

Huang, C. C., & Cheng, J. H. (2004). An investigation into the forming limits of sintered porous materials under different operational conditions. Journal of Materials Processing Technology, 148(3), 382-393.

Huang, C. C., & Cheng, J. H. (2005). A new forming-limit criterion for fracture prediction in a powder forging application. International journal of mechanical sciences, 47(7), 1123-1145.

Hyun-Joon J., Kwang S. L., Uta K., Jürgen E., Young W. C., Effect of crystalline phases on deformation and warm formability of a bulk metallic glass composite within super cooled liquid region. Materials Science and Engineering A 526 (2009) 62–68

Javadi, A., Cao, C., & Li, X. (2017). Manufacturing of Al-TiB_2 Nanocomposites by Flux-Assisted Liquid State Processing. Procedia Manufacturing: 10, 531-535.

Jiang, J., Chen, G., & Wang, Y. (2016). Compression mechanical behavior of 7075 aluminum matrix composite reinforced with nano-sized SiC particles in semisolid state. Journal of Materials Science & Technology, 32(11), 1197-1203.

Jiawen, F. M. C. X. H. (2009). Crack Initiation under Cyclic Compression. Journal of Materials Sciences and Technology, 5(5), 328-332.

Jiwei Geng, Tianran Hong, Yu Ma, MingliangWang, Dong Chen, Naiheng Ma, Haowei Wang (2016). The solution treatment of in-situ sub-micron TiB_2/2024 Al composite. Materials and Design 98 186–193

Khan, M., Rehman, A., Aziz, T., Naveed, K., Ahmad, I., & Subhani, T. (2017). Cold formability of friction stir processed aluminum composites containing carbon nanotubes and boron carbide particles. Materials Science and Engineering: A, 701, 382-388.

Kim, H. S., & Lee, D. N. (2004). Prediction of the forming limit of porous metals using the finite element method. Materials transactions, 45(6), 1829-1832.

Lee, M. S., Kim, S. J., Lim, O. D., & Kang, C. G. (2016). The effect process parameters on epoxy flow behavior and formability with CR340/CFRP composites by different laminating in deep drawing process. Journal of Materials Processing Technology, 229, 275-285.

Li, X., Liu, C., Luo, K., Ma, M., & Liu, R. (2016). Hot deformation behavior of SiC/AA6061 composites prepared by spark plasma sintering. Journal of Materials Science & Technology, 32(4), 291-297.

Liao, H., Wu, Y., Zhou, K., & Yang, J. (2015). Hot deformation behavior and processing map of Al–Si–Mg alloys containing different amount of silicon based on Gleebe-3500 hot compression simulation. Materials & Design (1980-2015), 65, 1091-1099.

Maron, B., Garthaus, C., Lenz, F., Hornig, A., Hübner, M., & Gude, M. (2016, October). Forming of carbon fiber reinforced thermoplastic composite tubes-Experimental and numerical approaches. In AIP Conference Proceedings (Vol. 1769, No. 1, p. 170028). AIP Publishing.

Meyer, B. C., Katsiropoulos, C. V., & Pantelakis, S. G. (2009). Hot forming behavior of non-crimp fabric peek/c thermoplastic composites. Composite Structures, 90(2), 225-232.

Munro, R. G. (2000). Material properties of titanium diboride. Journal of Research of the National Institute of Standards and Technology, 105(5), 709.

Narayan, S., & Rajeshkannan, A. (2017). Studies on formability of sintered aluminum composites during hot deformation using strain hardening parameters. Journal of materials research and technology, 6(2), 101-107.

Nezami, F. N., Gereke, T., & Cherif, C. (2017). Active forming manipulation of composite reinforcements for the suppression of forming defects. Composites Part A: Applied Science and Manufacturing, 99, 94-101.

Paweł H., Paweł K., Stanisław W., formability of AA6061/SiC composite at elevated temperatures. Material engineering (2015) 150-200

Poria S. G. Sutradhar, P. Sahoo (2017). Design of Experiments Analysis of Friction Behavior of Al-TiB_2 Composite. Materials Today: Proceedings 2956–2964

Pradeep Kumar G.S., R. Keshavamurthy, Prachi Kumari, Chirag Dubey (2016). Corrosion behavior of TiB_2 reinforced aluminum based in situ metal matrix composites. Perspectives in Science 8, 172-175

Suresh S., Shenbaga N., Vinayaga Moorthi (2013). Process development in stir casting and investigation on microstructures and wear behavior of TiB_2 on Al6061 MMC. Procedia Engineering 1183 – 1190

Talapatra, A., Agarwal, S. K., Pandit, S., Sengupta, A., & Saha, J. (2014). Formability characterization of composite sheet materials by Erichsen cupping testing method. International Journal of Chem Tech Research, 6(3), 1883-6.

Tian, X. (2018). Preparation and Forming Technology of Particle Reinforced Aluminum Matrix Composites. Insight-Material Science, 1(1).

Wang, W., Lowe, A., Davey, S., Zanjani, N. A., & Kalyanasundaram, S. (2015). Establishing a new Forming Limit Curve for a flax fibre reinforced polypropylene composite through stretch forming experiments. Composites Part A: Applied Science and Manufacturing, 77, 114-123.

Wolla, D. W., Davidson, M. J., & Khanra, A. K. (2014). Studies on the formability of powder metallurgical aluminum–copper composite. Materials & Design, 59, 151-159.

Wollmann, T., Hahn, M., Wiedemann, S., Zeiser, A., Jaschinski, J., Modler, N., & Paul, C. (2018). Thermoplastic fiber metal laminates: Stiffness properties and forming behavior by means of deep drawing. Archives of Civil and Mechanical Engineering, 18(2), 442-450.

Xianhui, W., Hao, Y., Shuhua, L., Mabao, L., & Qida, L. (2015). Effect of TiB particle size on erosion behavior of Ag-4wt% TiB_2 composite. Rare Metal Materials and Engineering, 44(11), 2612-2617.

7. APPENDIX

A. aluminum 1350 composition

MATERIAL	1350 EC GRADE ALUMINIUM ROD H14 (9.5MM)		
SPECIFICATION	ASTM B233		
ELEMENTS	MINIMUM	MAXIMUM	
% Si	–	0.100	
% Fe	–	0.250	
% Cu	–	0.020	
% Mn	–	0.010	
% Mg	–	0.020	
% Zn	–	0.030	
% Ti	–	0.020	
% Cr	–	0.010	
% Na	–	0.010	
% B	–	0.020	
% V	–	0.020	
% Ga	–	0.030	
OTHERS (EACH)	–	0.020	
OTHER (TOTAL)	–	0.100	
% AL	99.70	–	

ROD PROPERTIES		GRADE H12	
TENSILE	Mpa	83 - 110	
ELONGATION	% (250mm GL) Min	4.0	
RESISTIVITY	Ohm.mm²/m (Max)	0.028080	
CONDUCTIVITY	% IACS (Min)	61.5	

ROD COIL DIMENSIONS		Coefficient of linear expansion = 23 x 10^{-6}
COIL WEIGHT	: 2000 Kgs (±10%)	LINEAR WEIGHT = 191.74g/m
INTERNAL DIAMETER	: 570 mm	Density at 20°C = 2.703 kg/dm³
OUTER DIAMENTER	: 1390 mm	Melting point = 660 °C
COIL HEIGHT	: 890 mm	

REVIEWED BY: Mamur Faquirá

B. sample and its comparison test with UTM

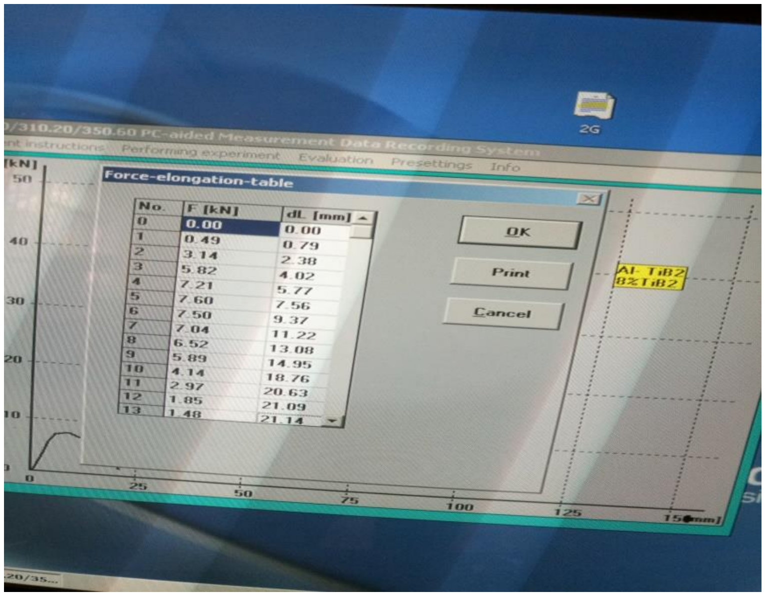

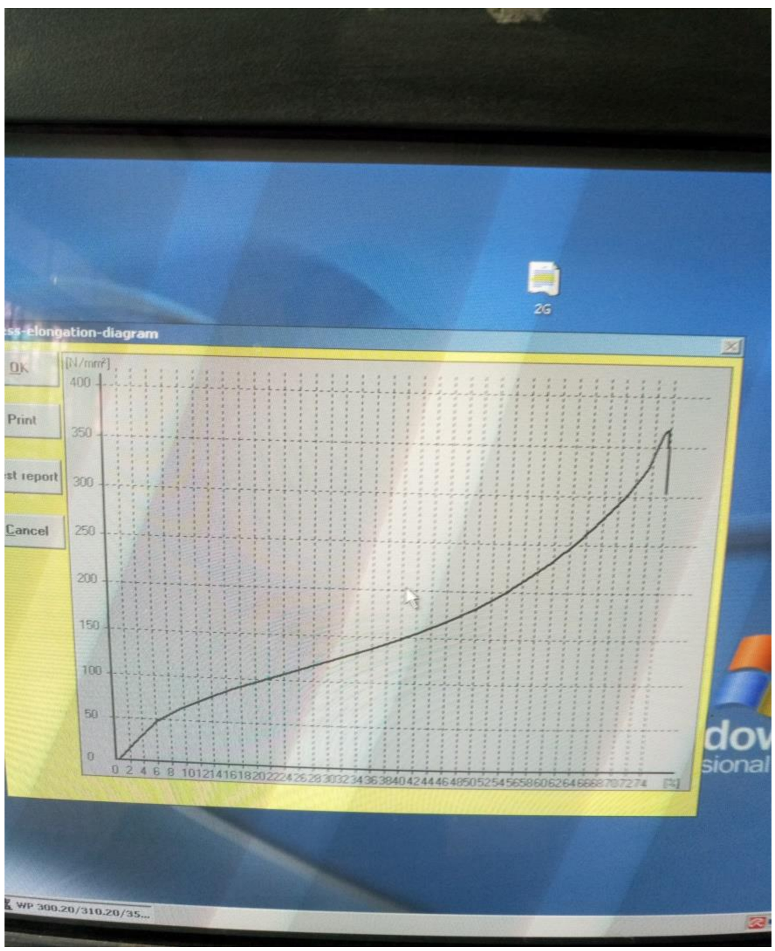

C. Micro hardness test in different percentage compossition

0%TiB_2 In 5kg.f

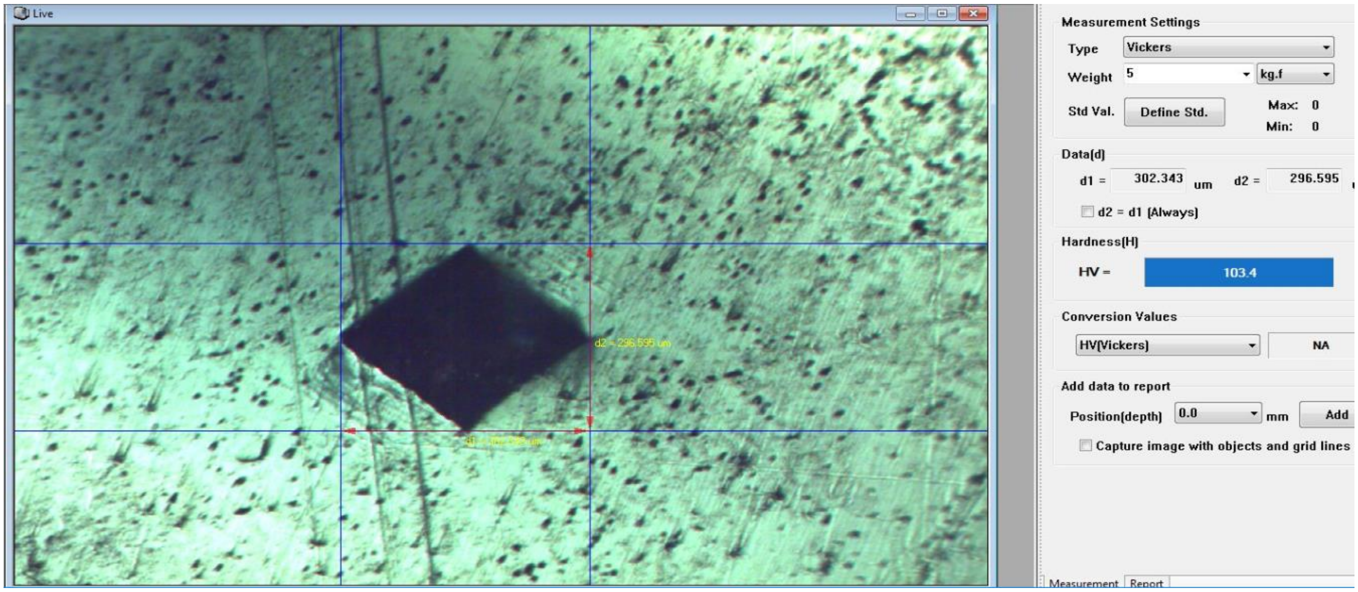

0%TiB_2 In 10kg.f

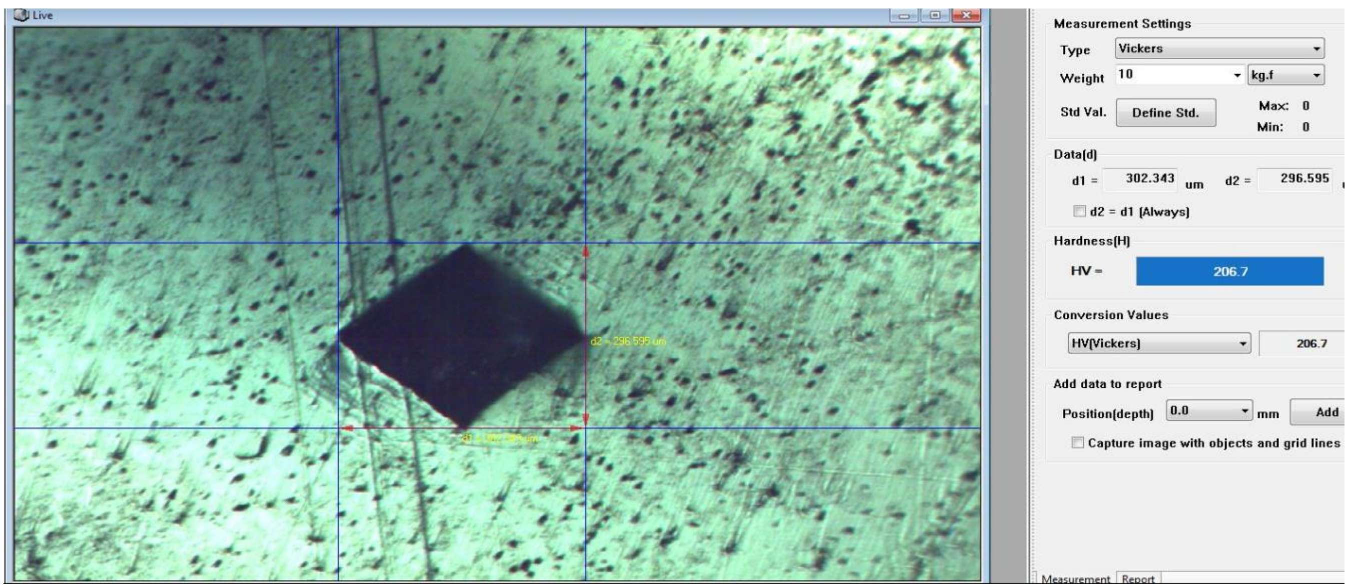

$12\%TiB_2$ In 10kg.f

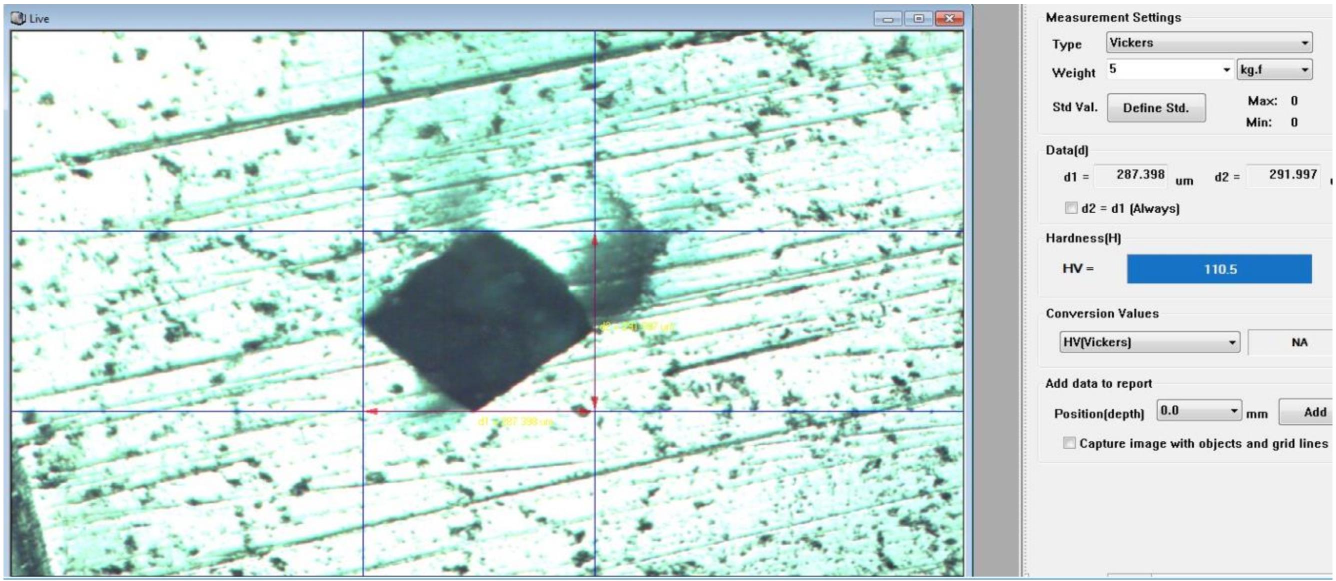

$4\%TiB_2$ In 10kg.f

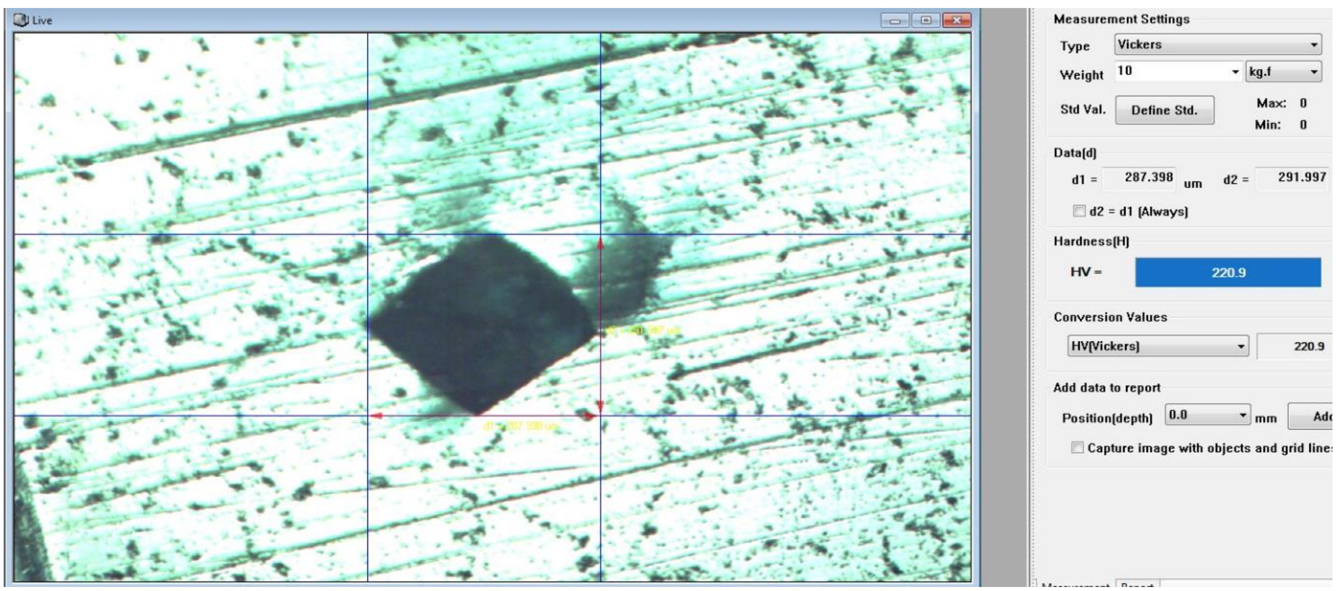

8%TiB_2 In 5kg.f

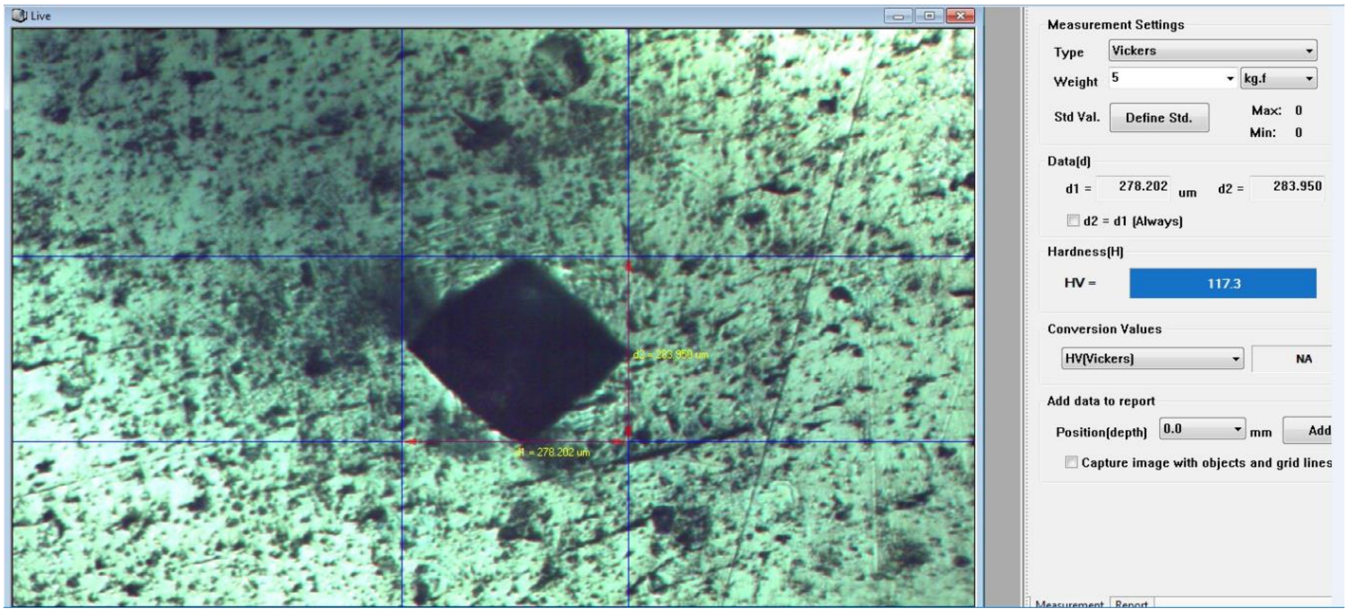

8%TiB_2 In 10kg.f

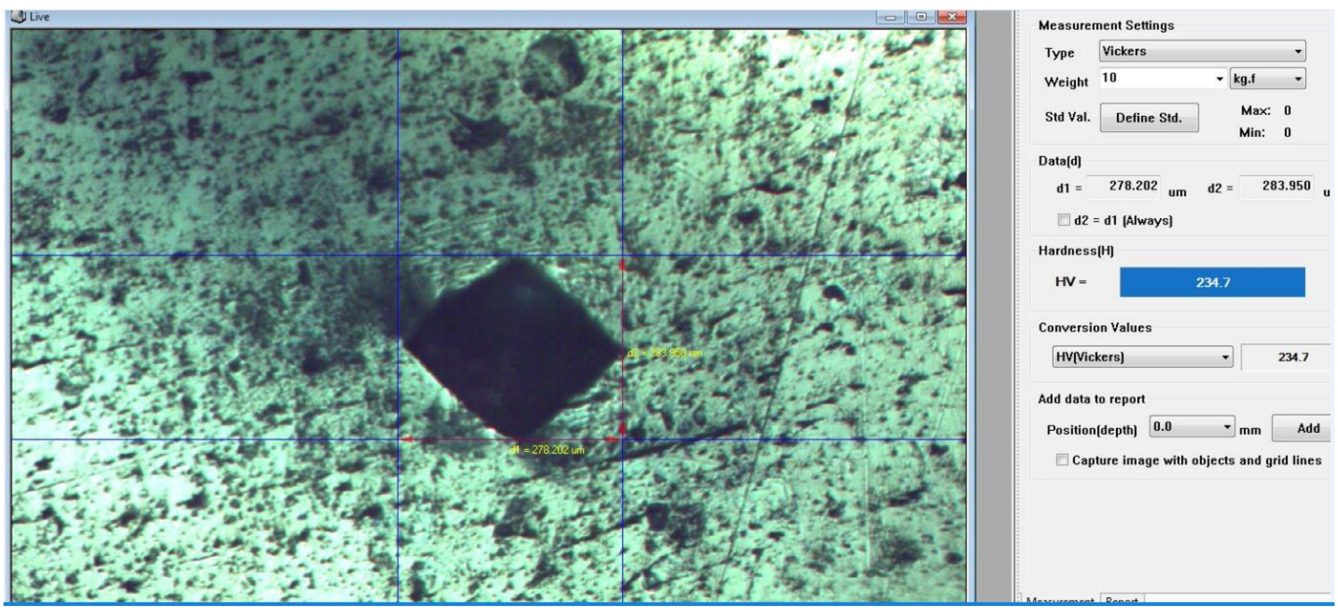

12%TiB_2
In 5kg.f

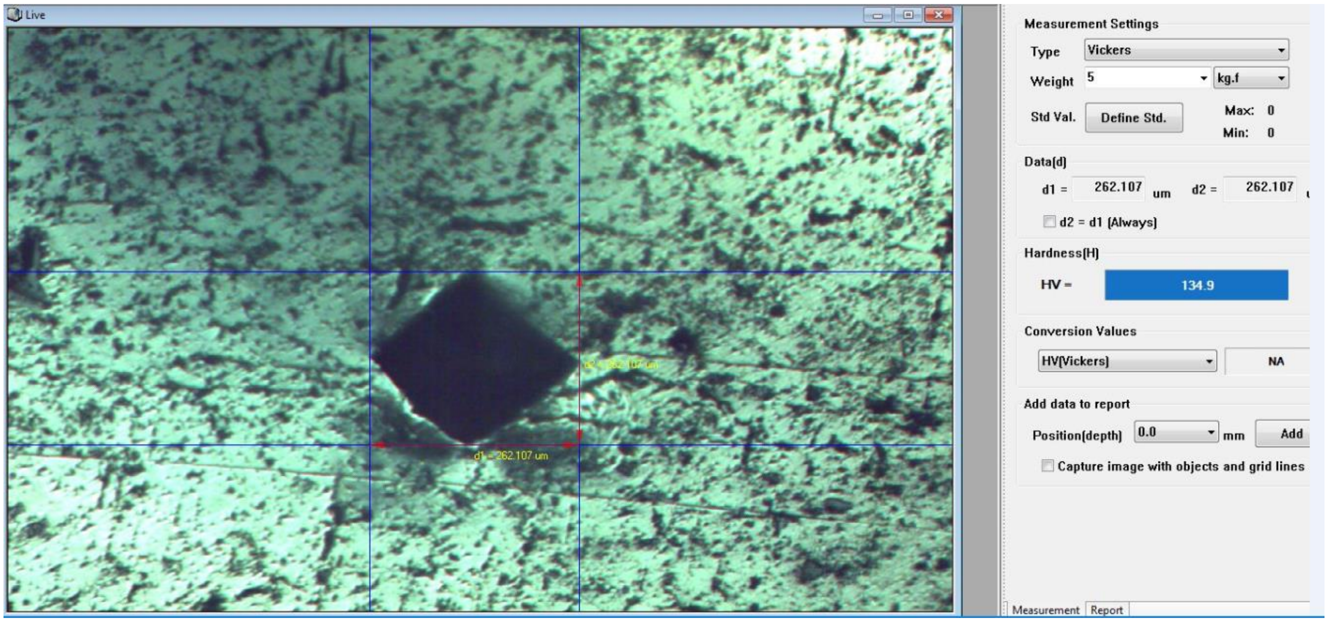

12%TiB_2
In 10kg.f